Journal of Medicinal Chemistry

pubs.acs.org/jmc

Article

Alkyl-Aryl-Vancomycins: Multimodal Glycopeptides with Weak Dependence on the Bacterial Metabolic State

Paramita Sarkar, Debajyoti Basak, Riya Mukherjee, Julia E. Bandow, and Jayanta Haldar*

Cite This: *J. Med. Chem.* 2021, 64, 10185−10202

Read Online

ACCESS | Metrics & More | Article Recommendations | Supporting Information

ABSTRACT: Resistance to last-resort antibiotics such as vancomycin for Gram-positive bacterial infections necessitates the development of new therapeutics. Furthermore, the ability of bacteria to survive antibiotic therapy through formation of biofilms and persister cells complicates treatment. Toward this, we report alkyl-aryl-vancomycins (AAVs), with high potency against vancomycin-resistant enterococci and staphylococci. Unlike vancomycin, the lead compound AAV-qC10 was bactericidal and weakly dependent on bacterial metabolism. This resulted in complete eradication of non-growing cells of MRSA and disruption of its biofilms. In addition to inhibiting cell wall biosynthesis like vancomycin, AAV-qC10 also depolarizes and permeabilizes the membrane. More importantly, the compound delocalized the cell division protein MinD, thereby impairing bacterial growth through multiple pathways. The potential of AAV-qC10 is exemplified by its superior efficacy against MRSA in a murine thigh infection model as compared to vancomycin. This work paves the way for structural optimization and drug development for combating drug-resistant bacterial infections.

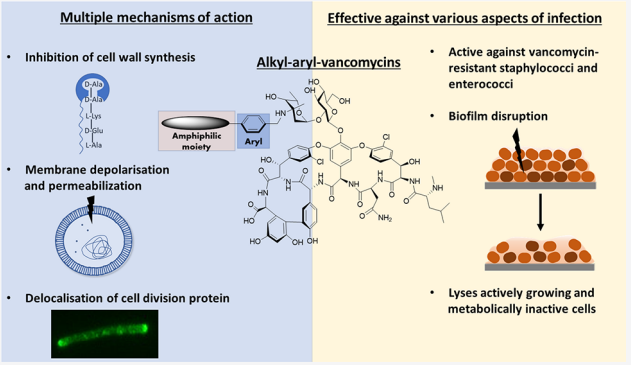

INTRODUCTION

Antimicrobial resistance is rapidly rendering blockbuster drugs obsolete. The situation is best exemplified by the emergence of enterococci and staphylococci resistant to vancomycin. This has prompted the World Health Organization (WHO) to list them as high-priority pathogens for antimicrobial drug discovery.[1] Coupled with the emergence of resistance to conventional antibiotics, chronic infections caused by *Staphylococcus aureus* are prone to relapses due to the formation of biofilms and persister cells.[2,3] Addressing these challenges for the effective treatment of bacterial infections also needs to be prioritized.[4]

Due to the clinical success of vancomycin before the report of resistance, continued drug discovery research toward glycopeptide antibiotics has led to the approval of three new second-generation glycopeptide antibiotics oritavancin, telavancin, and dalbavancin in the last decade.[5] Glycopeptide antibiotics act by binding to the D-Ala-D-Ala moiety of the pentapeptide stem of the peptidoglycan precursor.[6] This blocks the D-Ala-D-Ala moiety from interacting with transglycosylases and transpeptidases, impairing cell wall biosynthesis. A common feature of the second generation of antibiotics is an *N*-lipophile-substituted amino sugar, which imparts additional mechanisms of action in addition to D-Ala-D-Ala binding.[7] For example, telavancin is reported to inhibit lipid biosynthesis, while, in oritavancin, the liposaccharide entity can interact with and inhibit the transglycosylase enzymes that mediate polymerization of the cell wall precursors.[8] To date, numerous resistant phenotypes with variable susceptibility to each of the glycopeptide antibiotics have been reported.[9] The spectrum of activity of these seemingly similar glycopeptides derivatives differ against various phenotypes of vancomycin-resistant enterococci in their mechanisms of action and pharmacological properties, leaving room for further exploration.[8]

The bacterial cell envelope consisting of the cell wall and membrane constitutes various proteins essential for cell survival.[10] It serves as a protective barrier and is an excellent target for killing bacteria.[11] Antimicrobial peptides produced by the immune system also act by disrupting the membrane of *S. aureus*.[12] Drawing inspiration from the antimicrobial peptides, research groups have developed membrane-disruptive derivatives to overcome resistance to vancomycin.[5] Peripheral modifications on vancomycin to incorporate membrane-disruptive moieties have been explored.[13−16] Other strategies developed involve the enhancement of

Received: March 15, 2021
Published: July 7, 2021

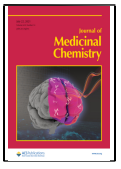

Scheme 1. Synthesis of Alkyl/Aryl-Aryl-Vancomycins

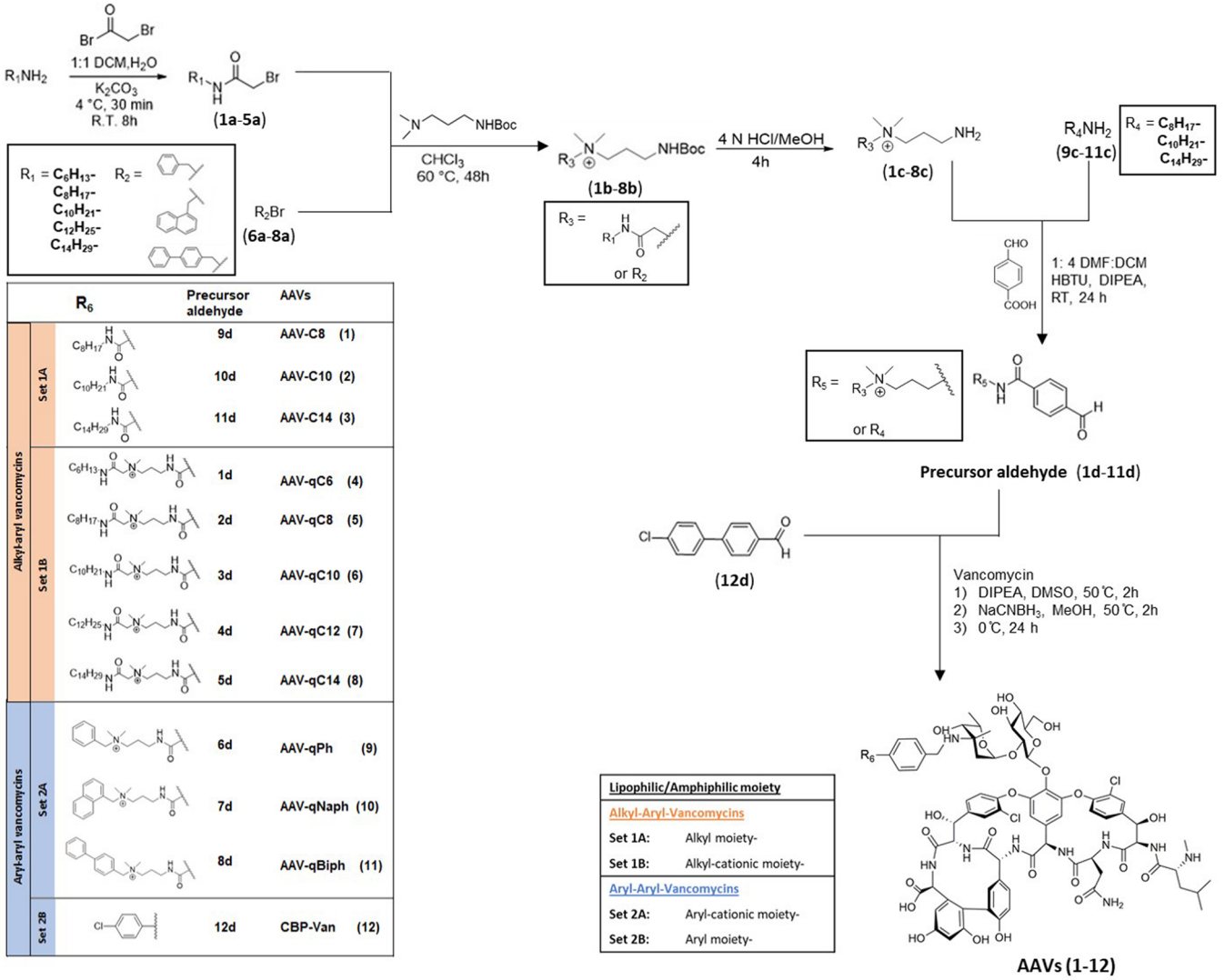

		R6	Precursor aldehyde	AAVs
Alkyl-aryl vancomycins	Set 1A	C_8H_{17}	9d	AAV-C8 (1)
		$C_{10}H_{21}$	10d	AAV-C10 (2)
		$C_{14}H_{29}$	11d	AAV-C14 (3)
	Set 1B	C_6H_{13}	1d	AAV-qC6 (4)
		C_8H_{17}	2d	AAV-qC8 (5)
		$C_{10}H_{21}$	3d	AAV-qC10 (6)
		$C_{12}H_{25}$	4d	AAV-qC12 (7)
		$C_{14}H_{29}$	5d	AAV-qC14 (8)
Aryl-aryl vancomycins	Set 2A		6d	AAV-qPh (9)
			7d	AAV-qNaph (10)
			8d	AAV-qBiph (11)
	Set 2B	Cl	12d	CBP-Van (12)

binding affinity to the target peptide or other components of the bacterial membrane;[17,18] and backbone modifications to substitute the lost binding affinity to the target.[19−21] However, vancomycin derivatives that overcome both genotypic and phenotypic resistance to vancomycin still remain underexplored. In a continued effort to develop more effective glycopeptide antibiotics to overcome both these aspects of infection, we report a class of alkyl-aryl-vancomycins (AAVs). In these molecules, the vancosamine sugar has been systematically functionalized with amphipathic moieties constituting aliphatic/aromatic groups with and without quaternary ammonium moieties. The effect of the compounds on bacteria at various stages of growth hinted at multiple mechanisms of action being at play. Systematic investigations deciphering the mode of action were undertaken. Finally, the efficacy of the best compound was validated in a murine model of infection.

RESULTS

Design and Synthesis. The second-generation glycopeptide antibiotics dalbavancin, oritavancin, and telavancin contain alkyl or aryl lipophilic substitutions on the sugar moieties of the glycopeptides. Dalbavancin is a derivative of the natural glycopeptide, teicoplanin containing a terminally branched dodecyl chain and is amidated at the carboxylic acid group.[22] Telavancin has a decylaminoethyl moiety conjugated at the vancosamine sugar and a methylaminophosphonic acid group at the resorcinol position.[22] This methylaminophosphonic acid group results in increased clearance and a reduction in kidney and liver distribution as compared with the derivative lacking it.[22] Oritavancin is a derivative of the naturally occurring glycopeptide chloroeremomycin containing a 4-chlorobiphenylmethyl moiety at the sugar and an additional 4-epivancosamine sugar. These variable modifications result in improved activity of the second-generation glycopeptides against vancomycin-resistant bacteria (VRB). We had also previously reported that C-terminus cationic lipophilic vancomycin derivatives were highly active against VRB.[23] Derivatives containing alkyl-, aryl-, and cationic moieties at the vancosamine sugar of vancomycin remain unexplored. Combinations of aromatic and aliphatic groups in various designs of antimicrobial agents have been shown to change the spectrum of activity and selectivity.[24,25] To explore this variation, broadly two sets of vancomycin derivatives with alkyl-aryl or aryl-aryl substitutions were synthesized, each consisting of subsets with and without a cationic moiety. We designed four sets of lipophilic/amphiphilic-aryl aldehyde precursors for derivatiza-

https://doi.org/10.1021/acs.jmedchem.1c00449
J. Med. Chem. 2021, 64, 10185−10202

Table 1. Antibacterial Activity of Alkyl/Aryl-Aryl-Vancomycins against Multidrug-Resistant Gram-Positive Bacteria and Toxicity against Human Erythrocytes (HC_{50})[a]

	MIC (μM)								HC_{50}
compounds	MRSA	VRSA 1	VRSA 4	VRSA 12	VRE 903	VRE 909	VRE ATCC 51575	VRE ATCC 51559	(μM)
AAV-C8 (**1**)	1	4.2	2.1	0.3	4.2	2.1	1	8.3	>250
AAV-C10 (**2**)	2	2	1	2	2	2	0.2	2	62.5
AAV-C14 (**3**)	4	8	4	4	2	4	4	4	27.5
AAV-qC6 (**4**)	0.4	14.9	29.8	7.4	7.4	14.9	>30	>30	>250
AAV-qC8 (**5**)	0.4	1.8	3.7	3.7	0.9	0.9	14.7	14.7	>250
AAV-qC10 (**6**)	0.9	1.8	0.45	0.9	0.45	0.9	3.6	3.6	>250
AAV-qC12 (**7**)	1.8	0.9	0.9	0.9	0.9	0.9	1.8	1.8	72
AAV-qC14 (**8**)	1.8	1.8	1.8	1.8	0.9	0.9	1.8	1.8	35
AAV-qPh (**9**)	0.9	30.5	30.5	30.5	>30	>30	>30	>30	>250
AAV-qNaph (**10**)	0.9	29.8	14.9	3.7	14.9	7.4	>30	>30	>250
AAV-qBiph (**11**)	0.5	7.3	7.3	3.7	7.3	3.7	14.7	14.7	>250
CBP-Van (**12**)	0.5	4.2	2.1	4.2	4.2	4.2	2.1	4.2	N.D
Vancomycin	0.6	346	346	346	692	346	346	1384	N.D

[a]MRSA, methicillin-resistant *S. aureus* ATCC 33591; VRSA, vancomycin-resistant *S. aureus;* VRE, vancomycin-resistant enterococci; and N.D., not determined.

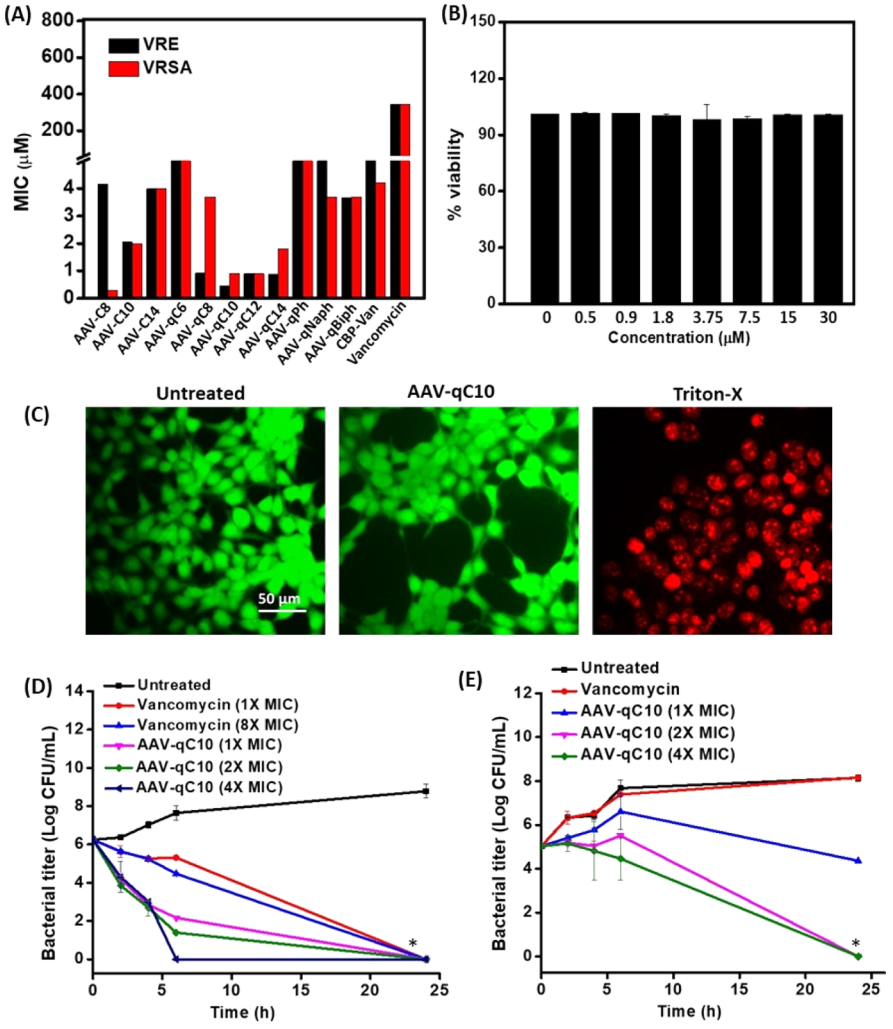

Figure 1. Antibacterial activity and cytotoxicity. (A) Trend of antibacterial activity of AAVs against VRE 909 and VRSA 4. (B) Viability of HEK cells upon treatment with AAV-qC10. (C) Microscopic images of HEK cells post-treatment with AAV-qC10 (30 μM) and 0.1% Triton-X and stained with calcein AM and propidium iodide (PI) dyes (scale bar for all images corresponds to 50 μm). Time-dependent bactericidal activity of vancomycin and AAV-qC10 against exponential growth phase drug-resistant (D) MRSA and (E) VRE (vancomycin was used at 64 μg/mL). "*" indicates <50 cfu/mL.

https://doi.org/10.1021/acs.jmedchem.1c00449
J. Med. Chem. 2021, 64, 10185−10202

tion of vancomycin at the primary amine of vancosamine through reductive amination (Scheme 1). In Set 1A (alkyl-aryl-vancomycins), an alkyl moiety (octyl-, decyl-, or tetradecyl-) was conjugated to 4-carboxy-benzaldehyde; Set 1B (aryl-alkyl-cationic-vancomycins) contained an amphiphilic moiety (alkyl-cationic moiety-), which includes a positive charge between the lipophilic group and the benzyl group, while Set 2A contains an aryl-cationic moiety conjugated to benzyl, as an appendage to vancomycin (Scheme 1). Set 2B consisted of one molecule with an aryl-aryl moiety (4-chlorobiphenyl-) conjugated to the vancosamine sugar (CBP-Van).

In the first step, alkyl amines (hexyl-, octyl-, decyl-, dodecyl-, and tetradecyl-amines) were reacted with bromoacetyl bromide in the presence of K_2CO_3 to yield activated bromides (**1a−5a**, Scheme 1). The tertiary amine of *tert*-butyl (3-(dimethylamino)propyl)carbamate was then reacted with respective activated alkyl bromides (**1a−5a**) and aryl bromides (benzyl-, naphthalen-1-yl-methyl-, and 4-chlorophenyl-benzyl bromides; **6a−8a**) to yield Boc-protected cationic-lipophilic intermediates **1b−8b**. This was followed by deprotection of the Boc-group under acidic conditions to generate primary amines bearing lipophilic-cationic intermediates (**1c−8c**). Then, the primary amine bearing lipophilic-cationic amines (**1c−8c**) and various alkyl amines (octyl-, decyl-, and tetradecyl-amines; **9c−11c**) was conjugated to the carboxylic acid of 4-carboxy-benzaldehyde through amide bond formation, using HBTU as a coupling agent, to obtain the precursor aldehydes (**1d−11d**). These aldehydes (**1d−11d**) and 4-chlorobiphenyl-carboxaldehyde (**12d**) were then conjugated with the primary amine of vancosamine of vancomycin by Schiff base formation, followed by reduction using $NaCNBH_3$ (reductive amination) to obtain the vancomycin derivatives (AAVs; **1−12**). All the derivatives of vancomycin were then purified by reversed-phase high-performance liquid chromatography (RP-HPLC) to more than 95% purity and characterized by high-resolution mass spectrometry (HRMS) and ^{1}H nuclear magnetic resonance (NMR) spectroscopy (Supporting Information).

In Vitro Antibacterial Activity. The antibacterial activity of the AAVs (**1−12**) was assessed as the minimum inhibitory concentration (MIC) against various vancomycin-resistant strains of staphylococci (VRSA) and enterococci (VRE), respectively. The MIC was determined as the lowest concentration of a compound required to completely inhibit the growth of bacteria. Vancomycin was inactive up to a concentration of 346 μM (512 μg/mL) against all vancomycin-resistant strains and showed an MIC of 0.7 μM against MRSA (Table 1). AAV-C8 showed 166-330-fold enhancement in activity against vancomycin-resistant strains (VRSA and VRE) and about 2-fold against vancomycin-sensitive strains (MRSA) as compared to vancomycin. The antibacterial activity increased in the decyl derivative AAV-C10 by up to 670-fold and 390-fold against VRE (MIC = 0.2−2 μM) and VRSA (MIC = 1−2 μM), respectively. The tetradecyl chain derivative (AAV-C14) exhibited 2- to 4-fold lower activity than the lower alkyl chain derivative, AAV-C10 (Figure 1A). The attachment of the alkyl-aryl moieties onto vancomycin (Set 1A: AAVs; **1−3**) resulted in the increased activity against VRB.

In Set 1B (alkyl-cationic-aryl-vancomycins, **4−8**), AAV-qC6 showed a 2-fold higher activity against MRSA, and 10- to 93-fold enhancement in activity against vancomycin-resistant pathogens (VRSA and VRE) as compared to vancomycin (Table 1). Substitutions with longer chains resulted in an increase in antibacterial activity. Against MRSA, the activity of AAV-qC8 was close to that of vancomycin, while against various strains of VRSA and VRE, an up to 750-fold increase in activity as compared to vancomycin was observed. The decyl-chain-containing derivative, AAV-qC10, showed an up to 1384-fold increase in activity against VRB as compared to vancomycin. An increase in the hydrophobicity beyond decyl did not result in a further enhancement in antimicrobial activity. Both AAV-qC12 and AAV-qC14 possessed similar activity, with up to 780-fold higher activity than vancomycin against VRB. These compounds had a similar trend of enhancement in activity against both VRE and VRSA (Figure 1A). The optimum activity was achieved by the decyl chain derivative AAV-qC10 (MIC_{VRE} = 0.45−3.6 μM and MIC_{VRSA} = 0.45−1.8 μM, Table 1). The introduction of alkyl-cationic-aryl moieties onto vancomycin in Set 1B also increased activity against both VRSA and VRE as compared to vancomycin and this enhancement was similar to that observed in Set 1A.

When the alkyl group of Set 1B was replaced with an aromatic group in Set 2A (aryl-cationic-aryl-vancomycins, **9−11**), the activity against VRE and VRSA was reduced. The phenyl-substituted derivative (AAV-qPh) was inactive up to 30 μM and the activity increased with the number of aromatic rings in AAV-qNaph and AAV-qBiph. The activity followed the order of AAV-qPh < AAV-qNaph < AAV-qBiph (Figure 1A). Among these, AAV-qBiph resulted in highest activity with 47−94-fold enhancement in activity against VRE and VRSA as compared to vancomycin (MIC = 3.7−14.7 μM). Although the compounds were more active than vancomycin against VRSA and VRE, the inclusion of aryl-cationic-aryl moieties also deterred the antimicrobial activity as compared to that of CBP-Van (Set 2B: aryl-aryl-vancomycin, **12**). CBP-Van showed activity similar to that of Set 1 against VRE and VRSA (MIC = 2−4 μM) but was more active than vancomycin against both VRE and VRSA. Overall, the compounds in Set 2A and Set 2B containing aryl-aryl substitutions were less active than a combination of alkyl-aryl substitutions in Set 1.

Given that the compounds in Set 1B showed highest activity, the activity of the cationic lipophilic portion of the most active compound, AAV-qC10, alone (Compound **13**, Scheme S1) and in combination with vancomycin was tested against vancomycin-resistant *Enterococcus faecium* (VRE). The MIC value of compound **13** was found to be > 40 μM against VRE. The physical mixture of vancomycin and compound **13** was inactive even up to their individual concentrations of 40 μM against VRE, whereas AAV-qC10 showed an MIC of 0.45 μM.

In Vitro Toxicity. *Toxicity against Human Erythrocytes (Hemolytic Activity).* For a drug candidate to be successful, it must exhibit low toxicity against mammalian cells. To assess the potential of these AAVs as drug candidates, the toxicity of the compounds was determined as their ability to lyse erythrocytes (50% hemolytic activity, HC_{50}). Among the Set 1A compounds, HC_{50} of AAV-C8 was greater than 250 μM, while AAV-C10 and AAV-C14 exhibited higher hemolytic activity with HC_{50} of 62.5 and 27.5 μM, respectively. An increase in hemolytic activity was observed with increasing hydrophobicity. The compounds in Set 1B, AAV-qC6, AAV-qC8, and AAV-qC10, displayed low hemolytic activity (1−12%) at 250 μM. However, a sharp increase in hemolytic activity was observed for the longer alkyl substitutions as in AAV-qC12 (HC_{50} = 72 μM) and AAV-qC14 (HC_{50} = 35 μM). In general, the compounds in Set 1B exhibited higher antibacterial activity than those in Set 1A and were also less

https://doi.org/10.1021/acs.jmedchem.1c00449
J. Med. Chem. 2021, 64, 10185−10202

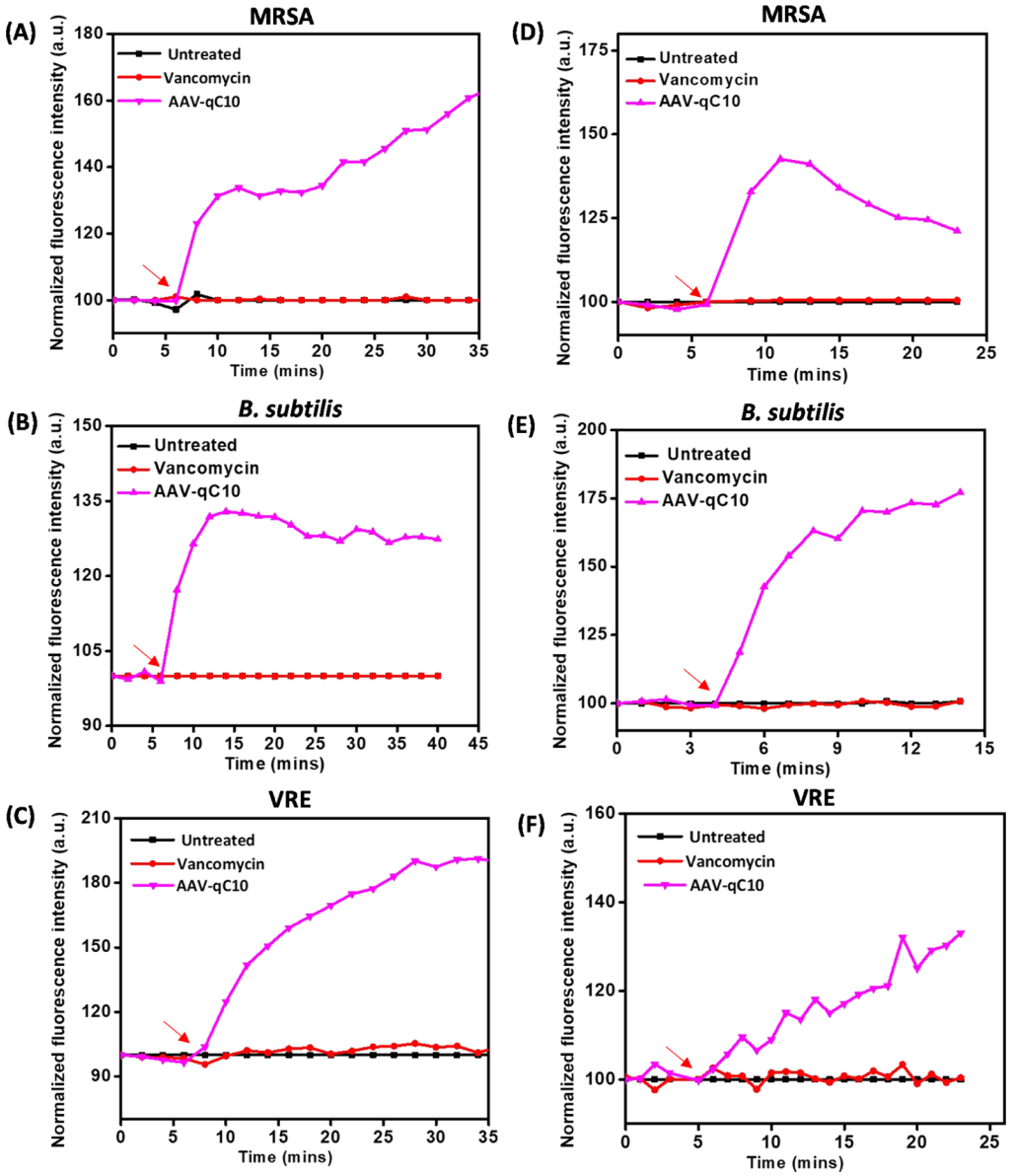

Figure 2. Study of the kinetics of (A−C) membrane depolarization and (D−F) membrane permeabilization of exponential phase MRSA, *B. subtilis*, and VRE by AAV-qC10 upon treatment at 10 μM concentration. Compound addition is indicated with arrows.

toxic to human erythrocytes. The aryl-cationic-aryl-substituted compounds in Set 2A exhibited moderate antibacterial activity and were also non-hemolytic up to 250 μM (0−2%). Based on the in vitro antibacterial and hemolytic activities, AAV-qC10 was selected as the optimum compound and was taken forward for further investigation.

Toxicity against the Human Embryonic Kidney Cell Line. In the alamarBlue assay, HEK cells treated with AAV-qC10 at various concentrations in the range of 0.5−30 μM were found to retain 100% viability (Figure 1B,C). Additionally, live−dead staining with calcein AM (AM—acetoxymethyl) and propidium iodide (PI) showed that none of the cells were stained with PI indicating that the compound showed no significant cytotoxicity.

Kinetics of Bactericidal Activity against Exponentially Growing Bacteria. The bactericidal activity of AAV-qC10 was tested against both vancomycin-sensitive bacteria (MRSA) and VRB (VRE) (Figure 1D,E). 6.1 log cfu/mL of MRSA was incubated with vancomycin (MIC, 8× MIC) and AAV-qC10 (MIC, 2× MIC and 4× MIC), and the bacterial titer over time was determined through spot plating (Figure 1D). Against MRSA, the MBC of AAV-qC10 was at MIC (0.9 μM). Irrespective of the concentration for AAV-qC10 treatment, a 2 log cfu/mL and 3 log cfu/mL reduction in bacterial titer was observed 2 and 4 h post-treatment. The bacterial titer gradually decreased, showing a 4.3 log cfu/mL reduction in 6 h and complete eradication (~6 log cfu/mL reduction) in 24 h at 2 ×MIC. Upon treatment at 4×MIC, the compound completely eradicated viable cells within 6 h. Thus, AAV-qC10 shows a concentration- and time-dependent bactericidal activity against MRSA. Vancomycin, on the other hand, exhibited a much slower time-dependent bactericidal activity against MRSA, maintaining a static effect on bacterial growth up to 6 h; and complete eradication was observed at 24 h and at all treatment concentrations.

Furthermore, the bactericidal kinetics of AAV-qC10 was tested against VRE. Bacteria (5 log cfu/mL) were incubated with AAV-qC10 at MIC, 2× MIC, and 4× MIC. Bacterial

https://doi.org/10.1021/acs.jmedchem.1c00449
J. Med. Chem. 2021, 64, 10185−10202

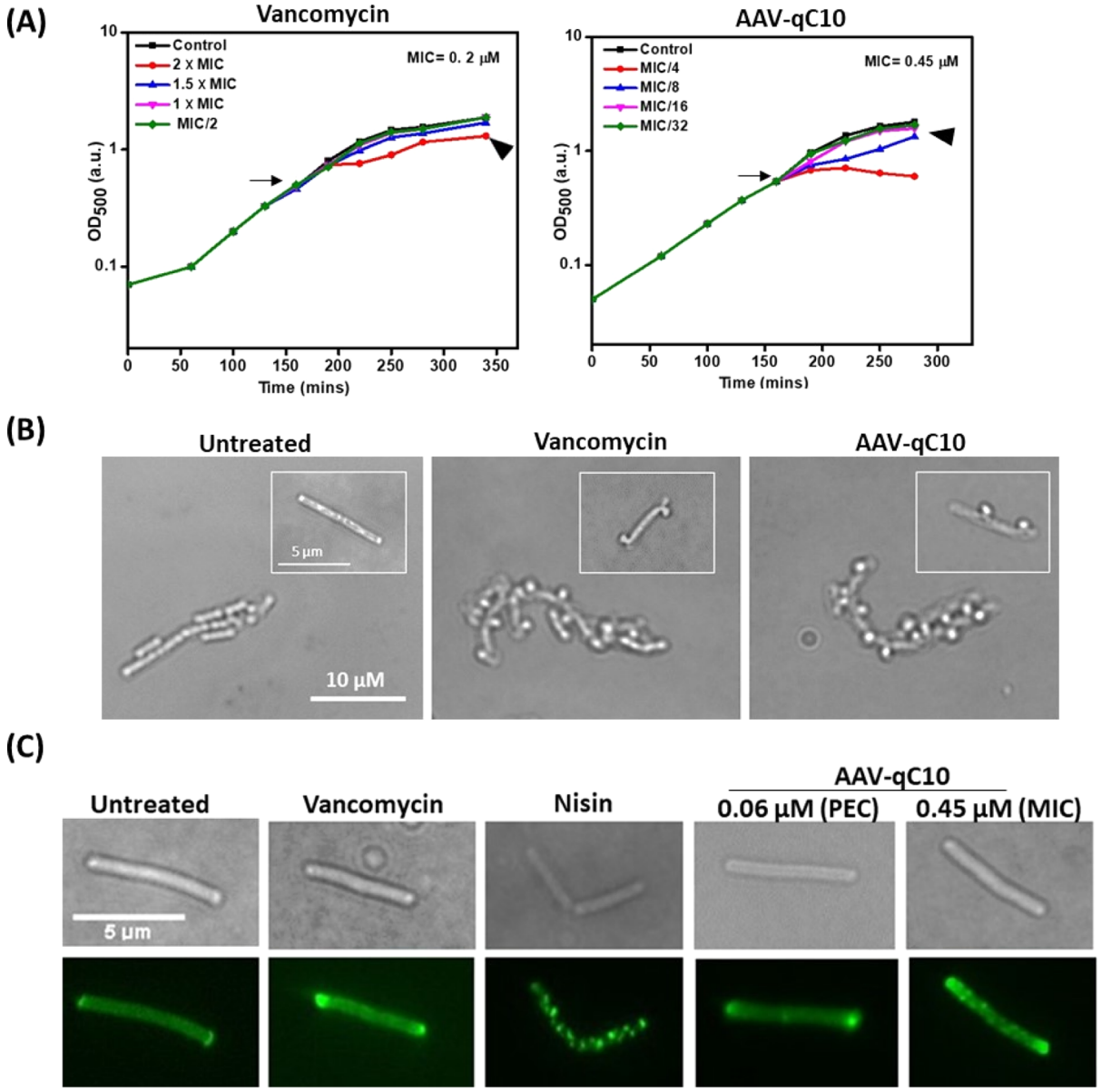

Figure 3. Examination of the mechanism of action in*B. subtilis.* (A) Growth retardation in early mid-log phase *B. subtilis* upon treatment with varying concentrations of vancomycin and AAV-qC10 (long arrows indicate compound addition and bold arrow heads indicate PECs). (B) Inhibition of cell wall biosynthesis at respective PECs by vancomycin (0.4 μM) and AAV-qC10 (0.06 μM) is indicated by extrusions (single-cell view in the inset). (C) Delocalization of the GFP-tagged MinD protein by vancomycin at PEC, nisin (0.75 μg/mL) and by AAV-qC10 at PEC and MIC.

growth was observed for 6 h upon exposure at MIC and 2× MIC. At 24 h postincubation, the viability of the bacteria was reduced by 0.7 log cfu/mL at MIC and complete eradication (5 log cfu/mL reduction) at 2× MIC (Figure 1E). Treatment at 4× MIC resulted in a 0.5 log cfu/mL reduction 6 h postincubation, and complete eradication (5 log cfu/mL reduction) at 24 h postincubation. AAV-qC10 was, therefore, found to be bactericidal against both MRSA and VRE.

Mechanisms of Action. *Antagonization assay.* Antagonization assay with *N*,*N*′-diacetyl-L-Lys-D-Ala-D-Ala and teichoic acid: In order to understand the contribution of other mechanisms of action, the change in MIC in the presence of excess of *N*,*N*′-diacetyl−L-Lys−D-Ala−D-Ala (KAA) was observed against MRSA. KAA, which corresponds to the target peptide of the glycopeptide antibiotics, would act as a competitive ligand and could, therefore, antagonize antibacterial activity. The tripeptide KAA at 500 μM could not antagonize the activity of AAV-qC10 and the MIC remained unchanged (MIC = 0.9 μM). However, the addition of the same amount of KAA could reduce the antibacterial activity of vancomycin from 0.6 μM to >30 μM (>40-fold change in MIC). This indicated that AAV-qC10 exhibited antibacterial activity through additional mechanisms of action, which are independent of target peptide binding. Given the presence of a cationic moiety in AAV-qC10, it is expected to interact with the negatively charged components of the bacterial cell wall. C-terminal trimethyl ammonium-modified vancomycin derivatives have been reported to bind to teichoic acid.[26] To test whether AAV-qC10 binds to teichoic acids, its MIC against MRSA in the presence of lipoteichoic acid (100 μg/mL) as a competing ligand was tested. No change in the MIC was observed in both vancomycin and AAV-qC10.

https://doi.org/10.1021/acs.jmedchem.1c00449
J. Med. Chem. 2021, 64, 10185−10202

Ability to Depolarize the Membrane of Bacteria.[23] The ability of AAV-qC10 to depolarize the membrane of MRSA, VRE and *Bacillus subtilis* were studied using the fluorescent probe DiSC3(5) (3,3′-dipropylthiadicarbocyanine iodide). DiSC3(5) is sensitive to the membrane potential and as it accumulates in the membrane, the fluorescence intensity decreases due to self-quenching. Upon disruption of the membrane potential, an increase in fluorescence is observed due to DiSC3(5) being dispersed in the solution. To verify whether AAV-qC10 or vancomycin affects the fluorescence of DiSC3(5), its fluorescence was monitored over time in the presence of the antibiotics (Figure S1). Neither vancomycin nor the compound interfered with the fluorescence of the dye. Post-incubation of AAV-qC10 with bacteria, at 10 μM, the fluorescence due to the DiSC3(5) dye increased gradually over time (Figure 2A−C). The increase was more rapid in *B. subtilis* and MRSA as compared to VRE. Vancomycin treatment at the same concentration does not have any effect on the bacterial membrane.

Ability to Permeabilize the Bacterial Membrane. The kinetics of membrane permeabilization by AAV-qC10 was measured by the uptake of the PI dye. Intact membranes are impermeable for PI, but PI enters the cell and binds to the DNA when the membrane integrity is compromised. The fluorescence of PI in a bacterial solution was measured for a few minutes before the addition of compounds at 10 μM each. Against MRSA and *B. subtilis*, AAV-qC10 showed a sharp increase in permeabilization, but against VRE, a slower membrane permeabilization was observed (Figure 2D−F). The differences in the extent of membrane permeabilization possibly result from differences in membrane composition among bacteria.

Growth Retardation in Early Mid-Log Phase B. subtilis and Cell Wall Biosynthesis Inhibition. The MIC of AAV-qC10 against *B. subtilis* was found to be 0.45 μM. For a better understanding of the mechanism of action of the compound, bacteria were treated at a concentration which allows bacterial cell proliferation, albeit inducing a stress response. This concentration is termed the physiologically effective concentration (PEC). To determine the PEC, bacterial cells were cultured to an OD_{500} of 0.35 (mid-log phase) and treated with compound at different concentrations to observe its acute effect on bacterial growth (Figure 3A). The PEC of AAV-qC10 was 0.06 μM. At higher concentrations, a decrease in the OD was observed, indicating growth arrest. Vancomycin, on the other hand, showed growth retardation only at 0.4 μM, which is 7-fold higher than that of AAV-qC10. To further investigate the mechanisms of action leading to growth retardation at the PEC, various microscopic studies were conducted with*B. subtilis*. Upon inhibition of a membrane-bound step in cell wall biosynthesis, new cell wall material is no longer incorporated into the cell wall. This leads to the formation of holes in the cell wall. Upon treatment of such compromised cells with a 1:3 mixture of acetic acid and methanol, the cytoplasmic membrane exudes out of these perforations, which appear as bubbles on the surface.[27] Upon treatment at the PEC, both vancomycin- and AAV-qC10-treated cells showed bubble-like formations on the bacterial cell surface, which indicated that they inhibit cell wall biosynthesis and compromise integrity of the wall (Figure 3B). Thus, inhibition of cell wall biosynthesis contributes to growth retardation by AAV-qC10 at the PEC. This may be the result of higher accumulation of the lipophilic derivative in the cell membrane region as compared to vancomycin, thereby enhancing ability to inhibit cell wall biosynthesis at a lower treatment concentration than vancomycin.

Delocalization of MinD Protein. The trans-membrane potential is crucial for the distribution and localization of the various cell division proteins such as MinD.[28] A disturbance of the membrane potential has implications in the functioning of the cell division machinery. The MinD protein localizes at the cell poles and upon delocalization, GFP-tagged-MinD appears as irregularly distributed spots throughout the cell surface. This is indicative of a compromised cell membrane.[28] To study the effect of the compounds on this cell division protein, microscopic studies were carried out by treating a GFP-MinD producing *B. subtilis* with vancomycin (at PEC = 0.4 μM) and AAV-qC10 (at PEC = 0.06 μM and at MIC = 0.45 μM). Nisin was used as a positive control for this experiment. It was found that AAV-qC10 did not delocalize the GFP-labeled MinD at PEC (Figure 3C). However, upon an increase in the concentration to 0.45 μM (MIC), 25% of the cells showed a delocalization. The results imply that membrane perturbation is not the predominant mechanism at the PEC and comes into play only at higher concentrations. Vancomycin, on the other hand, did not delocalize the MinD protein at the PEC (0.4 μM), which corresponds to 2× MIC. Nisin, which inhibits cell wall biosynthesis by obstructing lipid-II recycling and disrupts the bacterial membrane, shows a strong delocalization of the MinD protein at 0.75 μg/mL.

Membrane Disruption without Pore Formation. In addition to cell wall biosynthesis inhibition, and membrane depolarization, the compound was found to permeabilize the membrane of *B. subtilis* in the exponential growth phase (Figure 2D). To further study whether the membrane permeabilization by the compounds involved the formation of pores, bacteria were treated with antibiotics (vancomycin, AAV-qC10, and nisin as positive control) for 10 min and then observed microscopically postincubation with a mixture of the fluorescent dyes SYTO 9 and PI. In contrast to PI, which only stains permeabilized cells red, SYTO 9 is a membrane-permeable dye, and therefore stains both intact and permeabilized cells green. The antimicrobial peptide, nisin is known to disrupt bacterial membranes by forming pores.[29] Cells treated with nisin are stained by both SYTO 9 and PI, and therefore appear orange (Figure S2). Upon treatment with AAV-qC10 at PEC, around 5% of cells were stained with PI indicating that in a small fraction of the cells, the membranes are compromised to a degree that PI can penetrate the cell.

Bactericidal Activity against Metabolically Inactive Bacteria. The stationary phase and persister cells are metabolically inactive and have strongly reduced cellular processes. These cells are tolerant to antibiotic treatment and are major contributors to relapse and recurrence of disease. The bacterial membrane is essential for maintaining integrity and viability of the cells irrespective of the metabolic state. Compounds that disturb the membrane integrity are, therefore, effective against bacteria in various metabolic phases.[30] AAV-qC10 destabilizes the membrane through depolarization and permeabilization, in addition to other mechanisms of action such as cell wall biosynthesis inhibition and delocalization of cell division proteins. It was, therefore, expected that the compound would be effective against non-dividing cells as well. Antibiotics such as vancomycin and linezolid are inactive against stationary phase MRSA due to the lack of cell wall biosynthesis.[31] AAV-qC10 showed a

https://doi.org/10.1021/acs.jmedchem.1c00449
J. Med. Chem. 2021, 64, 10185−10202

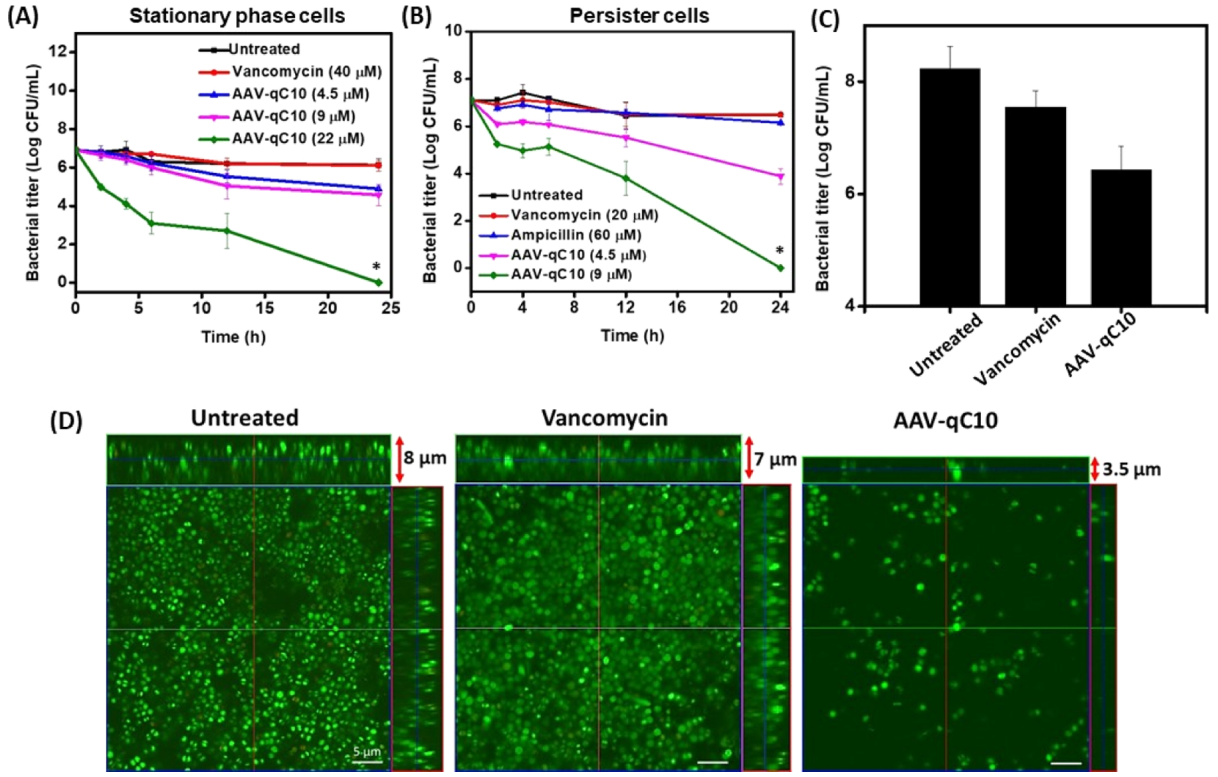

Figure 4. AAV-qC10 shows activity against biofilms and stationary and persister cells of MRSA. Kinetics of bactericidal activity against (A) stationary phase cells of MRSA and (B) persister cells of MRSA generated by 1 h treatment with 100 μg/mL ampicillin. (C) Viability of cells within the biofilm post-treatment with compounds. (D) Confocal microscopy imaging of biofilms of MRSA treated with vancomycin and AAV-qC10 at 20 μM, "*" indicates <50 cfu/mL.

concentration-dependent antibacterial activity against stationary phase cells of MRSA (Figure 4A). Around 7 log cfu/mL of bacteria were incubated with AAV-qC10 at various concentrations (4.5−22 μM). Treatment at 4.5 μM reduced the bacterial titer by 1.4 log cfu/mL and 2 log cfu/mL, 12 and 24 h post-treatment, respectively. At 9 μM, the compound showed a 1.9 log cfu/mL and 2.4 log cfu/mL reduction in bacterial titer 12 and 24 h post-treatment, respectively. Upon treatment at a higher concentration of 22 μM, a greater extent of reduction in bacterial titer was observed, with complete eradication (7 log cfu/mL reduction) after 24 h.

Persisters are a subpopulation of bacterial cultures that are refractory to antibiotic treatment and the stationary phase of *S. aureus* is known to be rich in persister cells.[32] Therefore, the activity of the compound against stationary phase bacteria warranted testing of its activity against persister cells generated by treating cultures with ampicillin.[32] The compound exhibited a more rapid antibacterial activity against persister cells than against stationary phase cells and a dose-sparing effect was observed in this case (Figure 4B). Treatment at 4.5 μM reduced the bacterial load by 1.6 log cfu/mL in 12 h and 3.3 log cfu/mL in 24 h. Treatment at a higher concentration of 9 μM resulted in a more rapid antibacterial activity with 2 log cfu/mL in 2 h and greater than 6 log cfu/mL reduction in 24 h. Treatment with ampicillin at 60 μM did not show any further reduction up to 24 h confirming that they were persister cells, and vancomycin at 40 μM was also ineffective against them for up to 24 h. The membrane-active nature of AAV-qC10 resulted in its activity against the metabolically inactive stationary phase and persister cells. This was evidenced by its membrane depolarization and permeabilization against these bacteria (Figure S3).

Activity against Bacterial Biofilms. A growing challenge in treating bacterial infections is the formation of biofilms, which are recalcitrant to antibiotic treatment.[33] The matrix of the biofilm acts as a protective barrier against antibiotics and the immune system.[34,35] Most antibiotics including vancomycin are rendered ineffective against biofilms consisting of both dividing and non-dividing cells. Thus, it is imperative to develop compounds that eradicate biofilms as well as planktonic cells. The viability of bacteria within biofilms treated with AAV-qC10 at 20 μM was reduced by 2.2 log cfu/mL as compared to the untreated control (Figure 4C). Vancomycin at the same concentration showed a 0.9 log cfu/mL reduction. Furthermore, microscopic examination of the mature biofilms of MRSA showed that they grew to a thickness of 8 μm, and treatment with vancomycin did not show a significant change, with a thickness of 7 μm. Biofilms treated with AAV-qC10 at 20 μM, on the other hand, were found to be uneven and have a reduced thickness of 3.5 μm (Figure 4D).

Postantibiotic Effect. The postantibiotic effect (PAE) is defined as the suppression of bacterial growth post-transient treatment with antibiotics.[36] It is the additional time required by the bacteria to recover from antibiotic treatment as compared to the untreated control. To study this, AAV-qC10 and vancomycin were incubated with 6.5 log cfu/mL of MRSA in the exponentially growing phase for 1 h. Post-treatment, the bacteria were washed to remove the antibiotic, resuspended in culture media, and allowed to grow at 37 °C. 1 h after treatment with vancomycin and AAV-qC10, and the

https://doi.org/10.1021/acs.jmedchem.1c00449
J. Med. Chem. 2021, 64, 10185−10202

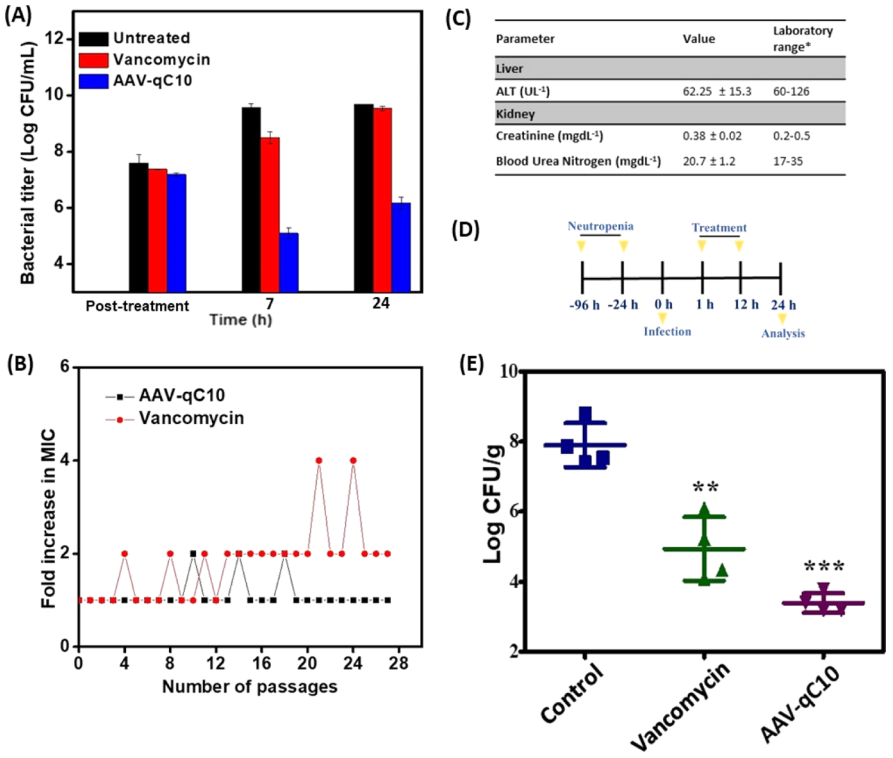

Figure 5. (A) Study of PAE of vancomycin and AAV-qC10 upon treatment at 10× MIC against MRSA. (B) Propensity of compounds to induce resistance in MRSA upon serial exposure to sub-MIC concentrations of vancomycin and AAV-qC10. (C) Effect of AAV-qC10 on the liver and kidney functional parameters in the blood of mice 48 h post-intraperitoneal treatment at 12 mg/kg (*Source: Charles River Laboratories). (D) Experimental design for in vivo efficacy study in the murine thigh infection model. (E) In vivo efficacy of AAV-qC10 and vancomycin against multidrug-resistant and methicillin-resistant *S. aureus* (MRSA) (n = 4/dose). Vancomycin and control vehicle were administered intraperitoneally twice at 12 h intervals at 12 mg/kg, and AAV-qC10 was administered intraperitoneally once 1 h postinfection at 12 mg/kg ("***" indicates $p <$ 0.0001 and "**" indicates $p <$ 0.001).

bacterial titer showed a 0.5 log cfu/mL and 0.8 log cfu/mL reduction, respectively (Figure 5A). The growth of the bacteria was then monitored at various time points post-incubation. In the vancomycin-treated group, 1 log cfu/mL increase in bacterial titer was observed 7 h post-removal of antibiotic stress (PAE = 6 h). Despite removal of AAV-qC10 stress, a 2 log cfu/mL reduction in viable cells was observed 7 h post-treatment. Further recovery of growth was observed at 24 h postremoval of antibiotic stress, indicating a prolonged PAE of 23 h at 10× MIC. Although the MIC of vancomycin and AAV-qC10 against MRSA is similar, the PAE is prolonged. Underlying causes might be a longer persistence of AAV-qC10 at the target site or the presence of additional mechanisms of action.

Propensity to Induce Resistance through Serial Passaging in MRSA. The potential of AAV-qC10 to induce resistance in MRSA was tested by serial exposure of bacteria to sub-MIC concentrations of the compound. After 27 passages, vancomycin showed a 2-fold increase in MIC against MRSA. However, no change in MIC of AAV-qC10 was observed after 27 passages (Figure 5B), indicating that the compound does not trigger spontaneous resistance development. The multimodal mechanisms of AAV-qC10 involving target peptide binding and membrane perturbation make resistance development even less frequent than for vancomycin.

Stability of AAV-qC10 in Plasma and Liver Homogenate. The protease stability of AAV-qC10 was evaluated by testing antibacterial activity post-incubation of the compound in 50% human plasma and 50% liver homogenate for 24 h. It retained activity (MIC = 0.9 μM) in both plasma as well as liver homogenate, thereby confirming resistance against protease degradation (Table S1).

In Vivo Toxicity and Activity. Treatment of mice through both intravenous and intraperitoneal routes at 55.5 mg/kg of AAV-qC10 was found to be well tolerated and all mice survived. Furthermore, no adverse toxicity effect on the liver or kidney was observed 48 h post-treatment with AAV-qC10 at 12 mg/kg (Figure 5C). The in vitro activity, the low toxicity at treatment concentrations, and the stability in mouse plasma and liver homogenate indicated the potential of AAV-qC10 for in vivo efficacy. The efficacy of AAV-qC10 was thus tested in a neutropenic mouse thigh infection model against MRSA. Neutropenic mice were infected with 5×10^5 cfu of MRSA per thigh. 1 h postinfection, vehicle control and vancomycin were administered intraperitoneally twice every 12 h at 12 mg/kg and a single 12 mg/kg dose of AAV-qC10 was given (Figure 5D). The mice were then sacrificed 24 h postinfection and the bacterial load in the infected thigh was determined. Prior to initiation of dosing (1 h postinfection), the bacterial load in the mice was determined to be 6.3 log cfu/g. In the vehicle-treated control group, 24 h postinfection, the bacterial load increased by a further 1.6 log cfu/g. Vancomycin treatment resulted in a 1.5 log cfu/g reduction in bacterial load as compared to the pretreatment bacterial load (Figure 5E). However, one dose of AAV-qC10 exhibited a significant reduction of 2.8 log cfu/g in bacterial load. Although the MIC values of vancomycin and AAV-qC10 are similar, the two antibiotics differ in their antibacterial properties such as longer PAE and more rapid

https://doi.org/10.1021/acs.jmedchem.1c00449
J. Med. Chem. 2021, 64, 10185−10202

bactericidal activity. Additionally, the pharmacological properties of AAV-qC10 could possibly be improved due to the presence of the amphiphilic moiety, as observed previously in the case of other lipophilic vancomycin derivatives and the second-generation glycopeptide antibiotics.[8,37] These factors possibly result in the superior in vivo efficacy of AAV-qC10 as compared to the parent drug vancomycin.

DISCUSSION

The prevalence of genotypic and phenotypic resistance to vancomycin poses a major challenge to the successful treatment with vancomycin. Linezolid, quinupristin/dalfopristin, daptomycin, and tigecycline constitute alternate treatments for infections with VRB.[38] However, resistance to even these antibiotics have been reported.[39] Newer antimicrobial agents for these multidrug-resistant superbugs is thus an urgent requirement. The clinical success of the glycopeptide antibiotics has drawn significant attention from the scientific community.

To tackle VRB, alkyl/aryl-aryl-vancomycins were developed through a rational design approach exploring the variation of lipophilic/amphiphilic substituents (alkyl- and aryl-moieties with or without cationic charges, Scheme 1). Analysis of activity and toxicity profiles of the sets of amphiphilic substitutions on vancomycin developed showed that, (i) a combination of aromatic and alkyl moieties in the amphiphilic substitution was best suited for significantly improved antibacterial activity against vancomycin resistant bacteria and (ii) the presence of the quaternary ammonium moiety in compounds with similar lipophilicity reduced toxicity, while retaining antibacterial activity. This increase in selectivity can be attributed to the higher content of negatively charged lipids in the bacterial cells resulting in greater interaction with positively charged antibacterial agents as compared to the more neutral lipid composition in eukaryotic cells.[40] The alkyl-aryl vancomycins exhibited high activity against the high-priority pathogens, VRE and VRSA. The lead compound, AAV-qC10, was highly bactericidal, which resulted in a significantly lower bacterial load than vancomycin, in a murine thigh infection model against MRSA (Figure 5E).

Mechanistic studies indicated that the synergy of multiple mechanisms of action contributes to the antibacterial activity of lead compound AAV-qC10. It was found to retard growth of *B. subtilis* in the mid-log phase upon treatment at 0.06 μM (PEC), while vancomycin showed a similar effect at 0.4 μM (Figure 3A). The presence of the amphiphilic alkyl-cationic-aryl moiety contributes to growth retardation at lower concentrations as compared to vancomycin. Further studies of the acute effect on exponentially growing bacteria showed that at the PEC, AAV-qC10 could inhibit cell wall biosynthesis and compromise cell wall integrity similar to vancomcyin. At this concentration, neither vancomycin nor AAV-qC10 delocalized the cell division protein, MinD, and few AAV-qC10 treated cells were observed to be permeabilized. This indicates that membrane perturbation and MinD delocalization are not the primary contributors to growth arrest observed upon treatment at PEC. However, at 0.45 μM, the synergy of multiple mechanisms of action, namely, cell wall biosynthesis inhibition, membrane depolarization, permeabilization, and consequent delocalization of MinD protein could contribute to the antibacterial activity. AAV-qC10 caused depolarization of the membrane of cells in the exponential growth phase of both MRSA and VRE to a similar extent, but permeabilization was lower in VRE. While the MIC of vancomycin increased in the presence of the competing target cell wall peptide (KAA) against MRSA, the MIC of AAV-qC10 remained unchanged. This further supports that antimicrobial activity of AAV-qC10 results from a synergy of multiple mechanisms of action. AAV-qC10 showed no change in MIC upon addition of excess teichoic acid, which rules out strong binding to teichoic acids of the cell wall. Its superior antibacterial properties are further exemplified by the prolonged PAE. This could be the result of increased interaction with the membrane due to the amphiphilic moiety in addition to target peptide binding, and therefore delayed growth recovery in the bacteria post-treatment (Figure 5A). This also indicates that a lower frequency of dosage might be sufficient for treatment of infections without compromising the efficacy, but reducing the possibility of adverse side effects.

AAV-qC10 showed a concentration- and time-dependent bactericidal activity against both staphylococci and enterococci in the exponential growth phase (Figure 1D,E). This can be attributed to multiple synergistic mechanisms of action against bacteria in this phase. Upon entering the stationary phase, cell wall biosynthesis comes to a halt. Furthermore, the cell wall of bacteria is thicker in the stationary phase than in the exponential phase.[41] These factors render vancomycin ineffective against metabolically inactive bacteria. However, in the case of AAV-qC10, the membrane perturbation results in the activity against these metabolically inactive bacteria. Because the bacterial cell membrane is crucial for maintaining the integrity of the cell, disturbing the cell membrane hampers these major cellular processes crucial for bacterial survival. Its antibacterial activity is weakly dependent on the growth state, showing slower bactericidal activity against the stationary phase cells (Figure 4A,B). A more rapid activity was observed against persister cells, which were generated by treatment of stationary phase cells with high concentrations of ampicillin. This may be due to the nonlethal damage to the cell wall inflicted by ampicillin, which may render the bacteria more susceptible to AAV-qC10. A similar effect has been observed in persisters of *Escherichia coli* treated with colistin and aminoglycosides.[42] Additionally, AAV-qC10 could disrupt preformed mature biofilms of MRSA and reduce the number of viable cells within them to a greater extent than vancomycin (Figure 4C,D). The results showcase the ability of AAV-qC10 to overcome the noninherited mechanisms of resistance to antibacterial agents in the form of biofilms and metabolically inactive bacteria.

AAV-qC10 outperformed the parent drug vancomycin in various aspects including overcoming noninherited resistance, prolonged PAE, and faster bactericidal activity both in vitro and in vivo. Overall, the present work demonstrates the potential of AAVs as new additions to the glycopeptide class of antibiotics with potential for clinical translation.

EXPERIMENTAL SECTION

Materials and Methods. Chemical reagents were purchased from Sigma-Aldrich, TCI Chemicals, and Spectrochem, India, and used without further purification. Vancomycin for synthesis was purchased from Chem-Impex Int. Inc. All the reaction solvents of reagent grade were purchased from Spectrochem and SD Fine Chemicals. Chloroform for column chromatography was purchased from SD Fine chemicals and distilled prior to use. HPLC-grade acetonitrile was purchased from Spectrochem. Analytical thin layer chromatography (TLC) was performed on Merck TLC plates precoated with silica gel 60 F_{254} (250 μm thickness). Propidium iodide and 3,3′-dipropylth-

https://doi.org/10.1021/acs.jmedchem.1c00449
J. Med. Chem. 2021, 64, 10185−10202

iadicarbocyanineiodide [$DiSC_3$ (5)] were procured from Sigma-Aldrich. All final vancomycin derivatives were purified by RP-HPLC using 0.1% trifluoroacetic acid in water/acetonitrile (5−95%) as the mobile phase. HPLC purification was performed on a Shimadzu-LC 8 Å Liquid Chromatography instrument (C18 column, 10 mm diameter, 250 mm length) with UV detector monitoring at 270 nm. All the final compounds, **1**−**12**, were isolated with more than 95% purity. The NMR spectra were recorded using a Bruker AMX-400 (400 MHz for ^{1}H) spectrometer in deuterated solvents. The chemical shifts (δ) are reported in parts per million downfield from the peak for the internal standard TMS for ^{1}H NMR. HRMS were obtained using a 6538-UHD Accurate Mass Q-TOF LC−MS instrument. A TECAN (Infinite series, M200 pro) plate reader was used to measure absorbance in biological assays. HEK 293 cells were obtained from ATCC. Bacterial strain, MRSA ATCC 33591, and Enterococcal strains (VRE 51575 and VRE 51559) were obtained from ATCC (Rockville, MD). Clinical isolates of VRSA (VRSA1, VRSA4, and VRSA 12) and VRE (VRE NR30909 and VRE NR30903) were obtained as a gift from Central Drug Research Institute (CDRI). Cell culture media were purchased from Gibco and Himedia.

Animals. Specific pathogen-free BALB/c female mice (20−25 g) were used for in vivo studies. The animal experiments were approved by the Institutional Animal Ethics Committee (IAEC) of National Institute of Veterinary Epidemiology and Disease Informatics (NIVEDI), Bengaluru (881/GO/ac/05/CPCSEA), and performed as per the guidelines of Committee for the purpose of Supervision and Experiments on Animals (CPCSEA), Ministry of Environment and Forests, New Delhi. As per the standard protocol, the mice were placed in individually ventilated cages within a controlled environment. A systemic toxicity study was carried out at Jawaharlal Nehru Center for Advanced Scientific Research (JNCASR) following institutional ethical guidelines.

Synthesis and Characterization of Compounds. *General Procedure for the Synthesis of **1a**−**5a**.* Alkyl amine (2 g, 1 equiv) was dissolved in dichloromethane (DCM) and stirred at 4 °C. K_2CO_3 (1.5 equiv) was dissolved in 10 mL Millipore water and added to the alkyl amine solution. Bromoacetyl bromide (1.5 equiv) was then dissolved in dry DCM and added dropwise into the reaction mixture at 4 °C over 30 min. The reaction mixture was then stirred at room temperature for 8 h. The product was extracted in chloroform and the chloroform was evaporated under reduced pressure to obtain the pure product with 90−95% yield.

*2-Bromo-N-hexyl-ethanamide (**1a**).* Yield 95%; ^{1}H NMR (400 MHz, $CDCl_3$) δ/ppm: 6.53 (s, 1H; CONH), 3.87 (s, 2H; $COCH_2Br$), 3.29−3.24 (m, 2H; $CONHCH_2$), 1.56−1.49 (m,2H; $NHCH_2CH_2C_4H_9$), 1.29 (bs, 6H; $CH_2(CH_2)_3CH_3$), 0.89−0.86 (m, CH3, 3H). HRMS m/z: 222.0489 (observed), 222.0495 (calcd for $[M + H]^+$).

*2-Bromo-N-octyl-ethanamide (**2a**).* Yield 90%; ^{1}H NMR (400 MHz, $CDCl_3$) δ/ppm: 6.52 (s, 1H; NHCO), 3.86 (s, 2H; $COCH_2Br$), 3.29−3.24 (m, 2H; $CONHCH_2$), 1.55−1.48 (m, 2H; $CONHCH_2CH_2C_6H_{13}$), 1.29−1.26 (m, 10H; ($CH_{2(C8\ alkyl\ chain)}$)), 0.86 (t, J = 7.2 Hz, 3H; CH_3). HRMS m/z: 250.0807 (observed), 250.0878 (calcd for $[M + H]^+$).

*2-Bromo-N-decyl-ethanamide (**3a**).* Yield 97%; ^{1}H NMR (400 MHz, $CDCl_3$) δ/ppm: 6.52 (s,1H; NHCO), 3.87 (s, 2H; $COCH_2Br$), 3.27 (dd, J = 13.2 Hz, 7.2 Hz, 2H; $CONHCH_2$), 1.56−1.49 (m, 2H; $NHCH_2CH_2C_8H_{17}$), 1.25 (bs, 14H; $CH_{2(C10\ alkyl\ chain)}$), 0.87 (t, J = 7.2 Hz, CH_3, 3H). HRMS m/z: 278.1111 (observed), 278.1120 (calcd for $[M + H]^+$).

*2-Bromo-N-dodecyl-ethanamide (**4a**).* Yield 98%; ^{1}H NMR (400 MHz, $CDCl_3$) δ/ppm: 6.46 (s,1H; NHCO), 3.88 (s, 2H; $COCH_2Br$), 3.28 (dd, J = 13.2 Hz, 6.8 Hz, 2H; $CONHCH_2$), 1.53 (dd, J = 14.4 Hz, 7.2 Hz, 2H; $CONHCH_2CH_2C_{10}H_{21}$), 1.26 (m, 18H; $CH_{2(C10\ alkyl\ chain)}$), 0.88 (t, J = 6.8 Hz, 3H; CH_3). HRMS m/z: 306.1381 (observed), 306.1354 (calcd for $[M + H]^+$).

*2-Bromo-N-tetradecyl-ethanamide (**5a**).* Yield 97%; ^{1}H NMR (400 MHz, $CDCl_3$) δ/ppm: 6.47 (s,1H; NHCO), 3.88 (s, 2H; $COCH_2Br$), 3.28 (dd, J = 13.2 Hz, 7.2 Hz, 2H; $CONHCH_2$), 1.55−1.52 (m, 2H; $CONHCH_2CH_2C_{12}H_{25}$), 1.26 (m, 22H; $CH_{2(C14\ alkyl\ chain)}$), 0.88 (t, J = 6.8 Hz, 3H; CH_3). HRMS m/z: 334.3355 (observed), 334.3354 (calcd for $[M + H]^+$).

*General Procedure for the Synthesis of **1b**−**8b**.* Compounds **1a**−**5a** (2 equiv) or the respective aryl bromides (**6a**−**8a**) were dissolved in dry chloroform in a sealed tube and Boc-*N*,*N*-dimethyl propylamine (1 g, 1 equiv) was added to it. The reaction mixture was allowed to reflux for 48 h. The pure products were obtained by column chromatography ($CHCl_3$/CH_3OH) using Silica gel as aminium derivatives.

*3-((tert-Butoxycarbonyl)amino)-N-(2-(hexylamino)-2-oxoethyl)-N,N-dimethylpropan-1-aminium Bromide (**1b**).* Yield 70%; ^{1}H NMR (400 MHz, $CDCl_3$) δ/ppm: 8.85 (bs, 1H; $CONHC_6H_{13}$), 5.20 (s, 1H; NHBoc), 4.56 (s, 2H; $N^+CH_2CONHC_6H_{13}$), 3.68 (d, J = 7.6 Hz, 2H; $BocNH(CH_2)_2CH_2N^+$), 3.36 (s, 6H; $N^+(CH_3)_2$), 3.29−3.24 (m, 4H; BocNH-CH_2CH_2 and CONH−CH_2), 2.14−2.10 (m, 2H; $N^+CH_2CH_2CH_2NHBoc$), 1.62−1.54 (m, 2H; $CONHCH_2CH_2C_4H_9$), 1.44 (s, 9H; O−$C(CH_3)_3$), 1.30−1.26 (m, 6H; $CH_{2(C6\ alkyl\ chain)}$), 0.88 (t, J = 7.2 Hz, 3H; CH_3). HRMS ESI$^+$ m/z: 344.2938 (observed), 344.2908 (calcd for M^+).

*3-((tert-Butoxycarbonyl)amino)-N,N-dimethyl-N-(2-(octylamino)-2-oxoethyl)propan-1-aminium Bromide (**2b**).* Yield 65%; ^{1}H NMR (400 MHz, $CDCl_3$) δ/ppm: 8.89 (bs, 1H; $CONHC_8H_{17}$), 5.11 (s, 1H; NHBoc), 4.54 (s, 2H; $N^+CH_2CONHC_8H_{17}$), 3.65 (t, J = 8.0 Hz, 2H; $BocNH(CH_2)_2CH_2N^+$), 3.35 (s, 6H; $N^+(CH_3)_2$), 3.29−3.24 (m, 4H; $BocNHCH_2CH_2$ and $CONHCH_2$), 2.16−2.09 (m, 2H; $N^+CH_2CH_2CH_2NHBoc$), 1.57−1.55 (m, 2H; $-CONHCH_2CH_2C_6H_{13}$), 1.44 (s, 9H,$OC(CH_3)_3$), 1.33−1.26 (m, 10H; $CH_{2(C8\ alkyl\ chain)}$), 0.87 (t, J = 6.8 Hz, CH_3, 3H). HRMS ESI$^+$ m/z: 372.3255 (observed), 372.3221 (calcd for M^+).

*3-((tert-Butoxycarbonyl)amino)-N-(2-(decylamino)-2-oxoethyl)-N,N-dimethylpropan-1-aminium Bromide (**3b**).* Yield 68%; ^{1}H NMR (400 MHz, $CDCl_3$) δ/ppm: 8.86 (bs, 1H; $CONHC_{10}H_{21}$), 5.15 (s, 1H; NHBoc), 4.55 (s, 2H; $N^+CH_2CONHC_{10}H_{21}$), 3.67 (t, J = 8.0 Hz, 2H; $BocNH(CH_2)_2CH_2N^+$), 3.35 (s, 6H; $N^+(CH_3)_2$), 3.27 (t, J = 6.0 Hz, 4H; $BocNHCH_2CH_2$ and $CONHCH_2$), 2.14−2.10 (m, 2H; $N^+CH_2CH_2CH_2NHBoc$), 1.60−1.55 (m, 2H; $CONHCH_2CH_2C_8H_{17}$), 1.44 (s, 9H; $OC(CH_3)_3$), 1.33−1.35 (m, 14H; $CH_{2(C10\ alkyl\ chain)}$), 0.87 (t, J = 8.0 Hz, 3H; CH_3). HRMS ESI$^+$ m/z: 400.3591 (observed), 400.3534 (calcd for M^+).

*3-((tert-Butoxycarbonyl)amino)-N-(2-(dodecylamino)-2-oxoethyl)-N,N-dimethylpropan-1-aminium Bromide (**4b**).* Yield 70%; ^{1}H NMR (400 MHz, $CDCl_3$) δ/ppm: 8.85 (t, J = 5.6 Hz, 1H; NHBoc), 5.14 (s, 1H; $CONHC_{12}H_{25}$), 4.58 (s, 2H; $N^+CH_2CONHC_{12}H_{25}$), 3.68 (t, J = 8.0 Hz, 2H; $BocNH(CH_2)_2CH_2N^+$), 3.36 (s, 6H; $N^+(CH_3)_2$), 3.28−3.23 (m, 4H; $BocNHCH_2CH_2$ and $CONHCH_2$), 2.16−2.09 (m, 2H; $N^+CH_2CH_2CH_2NHBoc$), 1.6−1.55 (m, 2H; $CONHCH_2CH_2C_{10}H_{23}$), 1.44 (s, 9H; $OC(CH_3)_3$), 1.25 (bs, 18H; $CH_{2(C12\ aryl\ chain)}$), 0.87 (t, J = 8.0 Hz, 3H; CH_3). HRMS ESI$^+$ m/z: 428.3846 (M^+ observed), 428.3847 (M^+ calcd).

*3-((tert-Butoxycarbonyl)amino)-N,N-dimethyl-N-(2-oxo-2-(tetradecylamino)ethyl) propan-1-aminium Bromide (**5b**).* Yield 72%; ^{1}H NMR (400 MHz, $CDCl_3$) δ/ppm: 8.87 (bs,1H; $CONHC_{14}H_{29}$), 5.13 (s, 1H; -NHBoc), 4.57 (s, 2H; $N^+CH_2CONHC_{14}H_{29}$), 3.67 (t, J = 7.6 Hz, 2H; $BocNH(CH_2)_2CH_2N^+$), 3.36 (s, 6H; $N^+(CH_3)_2$), 3.29−3.24 (m, 4H; $BocNHCH_2CH_2$ and $CONHCH_2$), 2.14−2.10 (m, 2H; $N^+CH_2CH_2CH_2NHBoc$), 1.62−1.53 (m, 2H; $CONHCH_2CH_2C_{12}H_{25}$), 1.44 (s, $OC(CH_3)_3$, 9H), 1.25 (bs, $CH_{2(C14\ alkyl\ chain)}$, 22H), 0.88 (t, J = 7.2 Hz,CH_3, 3H). HRMS ESI$^+$ m/z: 456.4204 (M^+ observed), 456.4160 (M^+ calcd).

*N-Benzyl-3-((tert-butoxycarbonyl)amino)-N,N-dimethylpropan-1-aminium Bromide (**6b**).* Yield 69%; ^{1}H NMR (400 MHz, DMSO-d_6) δ/ppm: 7.56−7.50 (m, 5H; H_{Ar}), 6.96 (t, J = 5.6 Hz, 1H; H_{Ar}), 4.59 (s, 2H; $CH_{2(Ar)}N^+$), 3.27−3.23 (m, 2H; $N^+CH_2CH_2$), 3.02 (s, 2H; CH_2NHBoc), 2.98 (s, 6H; $N^+(CH_3)_2$), 1.93 (t, J = 8.0 Hz, 2H; CH_2CH_2NHBoc), 1.37 (s, 9H; $OC(CH_3)_3$). HRMS ESI$^+$ m/z: 293.2211 (observed), 293.2224 (calcd for M^+).

*3-((tert-Butoxycarbonyl)amino)-N,N-dimethyl-N-(naphthalen-1-ylmethyl)propan-1-aminium Bromide (**7b**).* Yield 66%; ^{1}H NMR (400 MHz, DMSO-d_6) δ/ppm: 8.53 (d, J = 7.2 Hz, 1H; CONH),

https://doi.org/10.1021/acs.jmedchem.1c00449
J. Med. Chem. 2021, 64, 10185−10202

8.15 (d, J = 8.0 Hz, 2H; H_{Ar}), 8.06 (d, J = 8.0 Hz, 2H; H_{Ar}), 7.82 (d, J = 7.2 Hz, 2H; H_{Ar}), 7.70−7.60 (m, 3H; H_{Ar}), 6.98 (t, J = 5.6 Hz, 1H; H_{Ar}), 5.06 (s, 2H; $CH_{2(Ar)}N^+$), 3.47−3.43 (m, 2H; BocNHCH_2CH$_2$), 2.99 (bs, 8H; $N^+(CH_3)_2$ and $CH_2CH_2N^+$), 1.98 (m, 2H; CH_2CH_2NHBoc), 1.38 (s, 9H; O−C(CH_3)$_3$). HRMS ESI$^+$ m/z: 343.2364 (observed), 343.2360 (calcd for M^+).

*N-([1,1′-Biphenyl]-4-ylmethyl)-3-((tert-Butoxycarbonyl)amino)-N,N-dimethylpropan-1-aminium Bromide (**8b**).* Yield 70%; ^{1}H NMR (400 MHz, $CDCl_3$) δ/ppm: 7.70 (d, J = 8.0 Hz, 2H; H_{Ar}), 7.64 (d, J = 8.0 Hz, 2H; H_{Ar}), 7.54 (d, J = 7.2 Hz, 2H; H_{Ar}), 7.46−7.38 (m, 3H; H_{Ar}), 5.54 (bs, 1H; NHBoc), 4.99 (s, 2H; $CH_{2(Ar)}N^+$), 3.73 (bs, 2H; CH_2NHBoc), 3.30 (bs, 8H; $N^+(CH_3)_2$ and $CH_2CH_2N^+$), 2.20−2.17 (m, 2H; CH_2CH_2NHBoc), 1.41 (s, 9H; O−C(CH_3)$_3$). HRMS ESI$^+$ m/z: 369.2419 (observed), 369.2437 (calcd for M^+).

*General Procedure for the Synthesis of **1c**−**8c**.* Compounds **1b**−**8b** were dissolved in 1:1 solution of 4 N HCl and methanol and the mixture was stirred at room temperature for 4 h. The solvents were then evaporated under reduced pressure to obtain a pure product in quantitative yield.

*3-Amino-N,N-dimethyl-N-(2-oxo-2-(hexylamino)ethyl)propan-1-aminium Chloride (**1c**).* ^{1}H NMR (400 MHz, CD_3OD) δ/ppm: 8.48 (bs, 1H; CONH), 4.15 (s, 2H; N^+CH_2CONH), 3.72 (t, J = 8.4 Hz, 2H; $NH_2(CH_2)_2CH_2N^+$), 3.33 (s, 6H; $N^+(CH_3)_2$), 3.25−3.21 (m,2H; CONHC$H_2C_5H_{11}$), 3.04 (t, J = 7.6 Hz, 2H; NH_2CH_2), 2.25−2.18 (t, 2H; $N^+CH_2CH_2CH_2NH_2$), 1.56−1.53 (m, 2H; CONHCH$_2$CH_2), 1.32(bs, 6H; $CH_{2(C6\ alkyl\ chain)}$), 0.90 (t, J = 6.8 Hz, 3H; CH_3). HRMS ESI$^+$ m/z: 244.2388 (observed), 244.2383 (calcd for M^+).

*3-Amino-N,N-dimethyl-N-(2-oxo-2-(octylamino)ethyl)propan-1-aminium Chloride (**2c**).* ^{1}H NMR (400 MHz, DMSO-d_6) δ/ppm: 8.64 (bs, 1H; CONH), 7.96 (bs, 1H; CH_2NH_2) 4.15 (s, 2H; N^+CH_2CONH), 3.72 (t, J = 8.4 Hz, 2H; $NH_2(CH_2)_2CH_2N^+$), 3.33 (s, 6H; $N^+(CH_3)_2$), 3.25−3.21 (m,2H; CONHCH_2), 3.04 (t, J = 7.6 Hz, 2H; NH_2CH_2), 2.25−2.18 (t,2H; $N^+CH_2CH_2CH_2NH_2$), 1.56−1.53 (m, 2H; CONHCH$_2$CH_2), 1.32(bs, 10H; $CH_{2(C8\ alkyl\ chain)}$), 0.90 (t, J = 6.8 Hz, 3H; CH_3). HRMS ESI$^+$ m/z: 272.2678 (observed), 272.2696 (calcd for M^+).

*3-Amino-N,N-dimethyl-N-(2-oxo-2-(decylamino)ethyl)propan-1-aminium Chloride (**3c**).* ^{1}H NMR (400 MHz, DMSO-d_6) δ/ppm: 8.75 (bs, 1H; CONH), 8.11 (bs, 3H; $CH_2NH_3^+$) 4.15 (s, 2H; N^+CH_2CONH), 3.62−3.58 (m, 2H; $NH_2(CH_2)_2CH_2N^+$), 3.20 (s, 6H; $N^+(CH_3)_2$), 3.11 (dd, J = 12.4 Hz, 6.4 Hz, 2H; CONHCH_2), 2.86 (t, J = 6.4 Hz, 2H; NH_2CH_2), 2.06−2.02 (m, 2H; $N^+CH_2CH_2CH_2NH_2$), 1.43 (bs, 2H; CONHCH$_2$CH_2), 1.25 (bs, 14H; $CH_{2(C10\ alkyl\ chain)}$), 0.86 (t, J = 6.8 Hz, 3H; CH_3). HRMS ESI$^+$ m/z: 300.3010 (observed), 300.3009 (calcd for M^+).

*3-Amino-N,N-dimethyl-N-(2-oxo-2-(dodecylamino)ethyl)-propan-1-aminium Chloride (**4c**).* ^{1}H NMR (400 MHz, DMSO-d_6) δ/ppm: 8.78 (t, J = 5.6 Hz, 1H; CONH), 8.15 (s, 3H; $CH_2NH_3^+$) 4.11 (s, 2H; N^+CH_2CONH), 3.63−3.59 (m, 2H; $NH_2(CH_2)_2CH_2N^+$), 3.20 (s, 6H; $N^+(CH_3)_2$), 3.11 (dd, J = 12.8 Hz, 6.8 Hz, 2H; CONHCH_2), 2.86 (t, J = 6.8 Hz, 2H; NH_2CH_2), 2.09−1.99 (m, 2H; $N^+CH_2CH_2CH_2NH_2$), 1.44−1.43 (bs, 2H; CONHCH$_2$CH_2), 1.24 (bs, 18H; $CH_{2(C12\ alkyl\ chain)}$), 0.85 (t, J = 6.8 Hz, 3H; CH_3). HRMS ESI$^+$ m/z: 328.3368 (observed), 328.3322 (calcd for M^+).

*3-Amino-N,N-dimethyl-N-(2-oxo-2-(tetradecylamino)ethyl)-propan-1-aminium Chloride (**5c**).* ^{1}H NMR (400 MHz, DMSO-d_6) δ/ppm: 8.78 (t, J = 5.6 Hz, 1H; CONH), 8.14 (bs, 3H; $CH_2NH_3^+$) 4.11 (s, 2H; N^+CH_2CONH), 3.62−3.59 (m, 2H; $NH_2(CH_2)_2CH_2N^+$), 3.20 (s, 6H; $N^+(CH_3)_2$), 3.11 (d, J = 6.0 Hz, 2H; CONHCH_2), 2.86 (s, 2H; NH_2CH_2), 2.06−2.03 (m, 2H; $N^+CH_2CH_2CH_2NH_2$), 1.43 (bs, 2H; CONHCH$_2$CH_2), 1.24 (bs, 22H; $CH_{2(C14\ alkyl\ chain)}$), 0.86 (t, J = 6.8 Hz, 3H; CH_3). HRMS ESI$^+$ m/z: 356.3681 (observed), 356.3635 (calcd for M^+).

*3-Amino-N-benzyl-N,N-dimethylpropan-1-aminium Chloride (**6c**).* ^{1}H NMR (400 MHz, DMSO-d_6) δ/ppm: 8.06 (s, 3H; NH_3^+), 7.60−7.52 (m, 5H; H_{Ar}), 4.57 (s, 2H; $CH_{2(Ar)}NMe_2^+$), 3.39−3.35 (m, 2H; $CH_2NMe_2^+$), 2.99 (s, 6H; $N^+(CH_3)_2$), 2.90 (s, 2H; $NH_2CH_2CH_2$), 2.13−2.09 (m, 2H; $NH_2CH_2CH_2$). HRMS (ESI$^+$) m/z: 193.3055 (Observed), 193.3060 (calcd for M^+).

*3-Amino-N,N-dimethyl-N-(naphthalen-1-ylmethyl)propan-1-aminium Chloride (**7c**).* ^{1}H NMR (400 MHz, DMSO-d_6) δ/ppm 8.53 (d, J = 8.4 Hz, 1H; H_{Ar}) 8.19 (d, J = 8.0 Hz, 2H; H_{Ar}), 8.10 (d, J = 8.0 Hz, 1H; H_{Ar}), 7.89 (d, J = 6.8 Hz, 1H; H_{Ar}), 7.74−7.64 (m, 3H; NH_2 & H_{Ar}), 5.12 (s, 2H; N^+CH_2CONH), 3.64−3.62 (m, 2H; $CH_2NMe_2^+$), 3.06 (s, 6H; $N^+(CH_3)_2$), 2.95 (bs, 2H; $NH_2CH_2CH_2$), 2.23 (bs, 2H; $NH_2CH_2CH_2$). HRMS (ESI$^+$) m/z: 243.1842 (observed), 243.1856 (calcd for M^+).

*N-([1,1′-Biphenyl]-4-ylmethyl)-3-amino-N,N-dimethylpropan-1-aminium Chloride (**8c**).* ^{1}H NMR (400 MHz, DMSO-d_6) δ/ppm: 7.98 (s, 3H; NH_3^+), 7.87 (d, J = 8.0 Hz, 2H; H_{Ar}), 7.77 (d, J = 7.2 Hz, 2H; H_{Ar}), 7.71 (d, J = 8.4 Hz, 2H; H_{Ar}), 7.56 (t, J = 7.6 Hz, 2H; H_{Ar}), 7.46 (t, J = 7.6 Hz, 1H; H_{Ar}), 4.63 (s, 2H; N^+CH_2CONH), 3.43−3.39 (m, 2H; $CH_2NMe_2^+$), 3.06 (s, 6H; $N^+(CH_3)_2$), 2.96−2.91 (m, 2H; $NH_2CH_2CH_2$), 2.18−2.1 (m, 2H; $NH_2CH_2CH_2$). HRMS (ESI$^+$) m/z: 269.2031 (observed), 269.2012 (calcd for M^+).

*General Protocol for the Synthesis of Precursor Aldehydes (**1d**−**11d**).* 4-Formyl-benzoic acid (3.33 mmol, 1 equiv) and DIPEA (16.7 mmol, 5.0 equiv) were dissolved in a 4:1 mixture of DCM/DMF. The reaction was cooled to 4 °C and HBTU (4 mmol, 1.2 equiv) was added. The respective amines (3.67 mmol, 1.1 equiv, **1c**−**11c**) were added to the reaction mixture and allowed to stir for 24 h at room temperature. Following this, the reaction mixture was diluted with DCM and washed sequentially with water, 1 N HCl solution, and aqueous saturated bicarbonate solution. The organic layer was dried over anhydrous sodium sulfate, filtered, and concentrated in vacuo. A pure product was obtained through column chromatography using silica as the stationary phase (gradient: 60−70% ethyl acetate/hexane).

*3-(4-Formylbenzamido)-N,N-dimethyl-N-(2-(hexylamino)-2-oxoethyl)propan-1-aminium Chloride (**1d**).* Yield 75%; ^{1}H NMR (400 MHz, $CDCl_3$) δ/ppm: 9.96 (s, 1H; CHO), 7.98 (d, J = 8.0 Hz, 2H; H_{Ar}),7.91 (d, J = 7.6 Hz, 2H; H_{Ar}), 7.27 (d, J = 6.4 Hz, 1H; NH), 7.01 (d, J = 4.8 Hz, 1H; NH), 3.94 (s, 2H; $COCH_2NMe_2^+$), 3.64−3.60 (m, 2H; $CH_2NMe_2^+$), 3.51 (d, J = 5.6 Hz, 2H; CH_2NH), 3.24 (s, 6H; $N^+(CH_3)_2$), 3.20−3.15 (m, 2H; NCH_2), 1.44 (d, J = 7.2 Hz, 2H; CH_2CH_2NHCO), 1.21 (s, 8H; $CH_{2(C6\ alkyl\ chain)}$), 0.86 (t, J = 6.8 Hz 3H; $CH_{3(C6\ alkyl\ chain)}$); IR(KBr pellet): υ 2919 (b), 2850 (b), 1698 (s), 1647 (s), 1545 (b), 1468 (s), 1217 (s), 836 (s), 753 (s) cm^{-1}. HRMS: (ESI$^+$) m/z 376.5128 (observed), 376.5124 (calcd for M^+).

*3-(4-Formylbenzamido)-N,N-dimethyl-N-(2-(octylamino)-2-oxoethyl)propan-1-aminium Chloride (**2d**).* Yield 70%; ^{1}H NMR (400 MHz, $CDCl_3$) δ/ppm: 9.96 (s, 1H; CHO), 7.89 (d, J = 8.0 Hz, 2H; H_{Ar}), 7.81 (d, J = 8.4 Hz, 2H; H_{Ar}), 7.27 (d, J = 6.4 Hz, 1H; NH), 7.01 (d, J = 4.8 Hz, 1H; NH), 3.94 (s, 2H; $COCH_2NMe_2^+$), 3.64−3.60 (m, 2H; $CH_2NMe_2^+$), 3.51 (d, J = 5.6 Hz, 2H; CH_2NH), 3.24 (s, 6H; $N^+(CH_3)_2$), 3.20−3.15 (m, 2H; NCH_2), 1.44 (d, J = 7.2 Hz, 2H; CH_2CH_2NHCO), 1.21 (s, 12H; $CH_{2(C8\ alkyl\ chain)}$), 0.86 (t, J = 6.8 Hz 3H; $CH_{3(C8\ alkyl\ chain)}$); IR (KBr pellet): υ 3425 (b), 3321 (b), 2929 (s), 2852 (s), 1689 (s), 1648 (s), 1542 (b), 1468 (s), 1289 (s), 1216 (s), 833 (s), 753 (s) cm^{-1}. HRMS: (ESI$^+$) 404.2872 (observed), 404.2908 (calcd for M^+).

*3-(4-Formylbenzamido)-N,N-dimethyl-N-(2-(decylamino)-2-oxoethyl)propan-1-aminium Chloride (**3d**).* Yield 68%; ^{1}H NMR (400 MHz, DMSO-d_6) δ/ppm: 10.09 (s, 1H; CHO), 8.82 (t, J = 6.0 Hz, 1H; NH), 8.43 (t, J = 5.6 Hz, 1H; NH), 8.02 (s, 4H; H_{Ar}), 4.00 (s, 2H; $COCH_2NMe_2^+$), 3.56−3.52 (m, 2H; $CH_2NMe_2^+$), 3.37−3.33 (m, 2H; CH_2NH), 3.19 (s, 6H; $N^+(CH_3)_2$), 3.07−3.02 (m, 2H; CH_2CH_2NHCO), 1.38 (t, J = 6.0 Hz, 2H; NCH_2), 1.22 (s, 16H; $CH_{2(alkyl\ chain)}$), 0.87 (t, J = 6.8 Hz 3H; CH_3); IR (KBr pellet): υ 3381 (b), 2921 (s), 2849 (s), 1706 (s), 1629 (s), 1543 (s), 1466 (s), 1374 (s), 1205 (s), 845 (b), 819 (s), 757 (s) cm^{-1}. HRMS: (ESI$^+$) 432.3186 (observed), 432.3221 (calcd for M^+).

*3-(4-Formylbenzamido)-N,N-dimethyl-N-(2-(dodecylamino)-2-oxoethyl)propan-1-aminium Chloride (**4d**).* Yield 65%;^{1}H NMR (400 MHz, $CDCl_3$) δ/ppm: 9.96 (s, 1H; CHO), 7.88 (d, J = 8.4 Hz, 2H; H_{Ar}), 7.81 (d, J = 8.0 Hz, 2H; H_{Ar}), 7.27 (d, J = 6.4 Hz, 1H; NH), 7.02 (d, J = 4.8 Hz, 1H; NH), 3.94 (s, 2H; $COCH_2NMe_2^+$), 3.62 (t, J

https://doi.org/10.1021/acs.jmedchem.1c00449
J. Med. Chem. 2021, 64, 10185−10202

= 8.4 Hz, 2H; $CH_2NMe_2^+$), 3.51 (d, J = 5.6 Hz, 2H; CH_2NH), 3.24 (s, 6H; $N^+(CH_3)_2$), 3.20−3.15 (m, 2H; NCH_2), 1.44 (d, J = 7.2 Hz, 2H; CH_2CH_2NHCO), 1.21 (s, 20H; $CH_{2(C12\ alkyl\ chain)}$), 0.86 (t, J = 6.8 Hz, 3H; $CH_{3(C12\ alkyl\ chain)}$); IR (KBr pellet): υ 3427 (b), 3324 (b), 2919 (s), 2850 (s), 1696 (b), 1647 (s), 1544 (b), 1468 (s), 1300 (s), 1217 (s), 835 (b), 753 (s) cm^{-1}. HRMS: (ESI^+) 460.3513 (observed), 460.3534 (calcd for M^+).

*3-(4-Formylbenzamido)-N,N-dimethyl-N-(2-oxo-2-(tetradecylamino)ethyl)propan-1-aminium Chloride (**5d**).* Yield 69%; ^1H NMR (400 MHz, $CDCl_3$) δ/ppm: 10.05 (s, 1H; CHO), 7.98 (d, J = 8.0 Hz, 2H; H_{Ar}), 7.91 (d, J = 7.6 Hz, 2H; H_{Ar}), 7.15 (s, 1H; NH), 6.96 (s, 1H; NH), 3.97 (s, 2H; $COCH_2NMe_2^+$), 3.58 (s, 4H; CH_2NH & $CH_2NMe_2^+$), 3.28 (s, 6H; $N^+(CH_3)_2$), 3.22 (d, J = 6.0 Hz, 2H; CH_2CH_2NHCO), 2.18 (d, J = 5.2 Hz, 2H; NCH_2), 1.24 (s, 24H; $CH_{2(C14\ alkyl\ chain)}$), 0.87 (t, J = 6.4 Hz, 3H; $CH_{3(C14\ alkyl\ chain)}$); IR (KBr pellet): υ 3427 (b), 3322 (b), 2919 (s), 2850 (s), 1695 (b), 1646 (s), 1545 (b), 1467 (s), 1322 (s), 1217 (s), 835 (b), 753 (s) cm^{-1}. HRMS: (ESI^+) 488.3833 (observed); 488.3847 (calcd for M^+).

*N-Benzyl-3-(4-formylbenzamido)-N,N-dimethylpropan-1-aminium Chloride (**6d**).* Yield 70%; ^1H NMR (400 MHz, $CDCl_3$) δ/ppm: 10.04 (s, 1H; CHO), 8.11 (d, J = 8.8 Hz, 2H; H_{Ar}), 7.96 (d, J = 8.0 Hz, 2H; H_{Ar}), 7.82 (d, J = 8.4 Hz, 2H; NH), 7.70−7.66 (m, 2H; H_{Ar}), 7.54−7.51 (m, 3H; H_{Ar}), 4.53 (s, 6H; $N^+(CH_3)_2$), 3.34 (d, J = 2.0 Hz, 2H; CH_2NH), 2.68 (s, 4H; $CH_{2(Ar)}NMe_2^+$& $CH_2NMe_2^+$), 1.21 (bs, 2H; $CH_2CH_2CH_2$); IR (KBr pellet): υ 3460 (b), 2919 (s), 2850 (s), 1712 (s), 1647 (s), 1543 (s), 1518 (s), 1483 (s), 1325 (s), 1271 (s), 1241 (s), 1162 (s), 1126 (s), 1068 (s), 1016 (s), 833 (s) cm^{-1}. HRMS: (ESI^+) 325.1903 (observed), 325.1911 (calcd for M^+).

*3-(4-Formylbenzamido)-N,N-dimethyl-N-(naphthalen-1-ylmethyl)propan-1-aminium Chloride (**7d**).* Yield 62%; ^1H NMR (400 MHz, $CDCl_3$) δ/ppm: 10.10 (s, 1H; CHO), 8.81 (t, J = 5.6 Hz, 1H; NH), 8.12 (d, J = 8.4 Hz, 2H; H_{Ar}), 8.02 (s, 4H; H_{Ar}), 7.96 (d, J = 8.4 Hz, 1H; HAr), 7.61−7.52 (m, 4H; H_{Ar}), 5.05 (s, 2H; $CH_{2(Ar)}NMe_2^+$), 3.52 (s, 6H; $N^+(CH_3)_2$), 3.01 (s, 2H; $CH_2NMe_2^+$), 2.68 (s, 2H; CH_2NH), 1.22 (bs, 2H; $CH_2CH_2CH_2$); IR (KBr pellet): υ 3413 (b), 3274 (b), 3002 (s), 2970 (s), 2920 (s), 1708 (s), 1647 (s), 1517 (s), 1466 (s), 1366 (s), 1274 (s), 1170 (s), 1076 (s), 884 (s), 819 (s), 746 (s) cm^{-1}. HRMS: (ESI^+) 375.2131 (observed), 375.2101 (calcd for M^+).

*N-([1,1′-Biphenyl]-4-ylmethyl)-5-(4-formylphenyl)-N,N-dimethyl-5-oxopentan-1-aminium Chloride (**8d**).* Yield 66%; ^1H NMR (400 MHz, $CDCl_3$) δ ppm: 10.08 (s, 1H; CHO), 8.84 (t, J = 5.6 Hz, 1H; NH), 8.03 (dd, J = 17.6 Hz, 8.0 Hz, 4H; H_{Ar}), 7.67 (d, J = 8.0 Hz, 2H; H_{Ar}),7.61−7.58 (m, 4H; H_{Ar}), 7.48−7.38 (m, 3H; H_{Ar}), 4.57 (s, 2H; $CH_{2(Ar)}NMe_2^+$), 3.42−3.39 (m, 2H; $CH_2NMe_2^+$), 3.02 (s, 6H; $N^+(CH_3)_2$), 2.13 (d, J = 7.6 Hz, 2H; CH_2NH), 1.08 (t, J = 7.2 Hz, 2H; $CH_2CH_2CH_2$); IR (KBr pellet): υ 3308 (b), 2979 (b), 1686 (s), 1542 (s), 1487 (b), 1365 (s), 1281 (s), 1249 (s), 1165 (s), 987 (s), 777 (s), 749 (s),697(s) cm^{-1}. MALDI-MS: 401.22 (observed), 401.2179 (calcd for M^+).

*4-Formyl-N-octylbenzamide (**9d**).* Yield 70%; ^1H NMR (400 MHz, $CDCl_3$) δ/ppm: 10.04 (s, 1H; CHO), 7.90 (s, 4H; H_{Ar}), 6.45 (s, 1H; NH), 3.46−3.41 (m, 2H; $NHCH_2$), 1.64−1.57 (m, 2H; CH_2), 1.34−1.25 (m, 10H; $5CH_2$), 0.086 (t, J = 7.2 Hz, 3H; CH_3); HRMS (ESI^+) m/z: 262.1816 (observed), 262.1802 (calcd for $[M + H]^+$).

*4-Formyl-N-decylbenzamide (**10d**).* Yield 72%; ^1H NMR (400 MHz, $CDCl_3$) δ/ppm: 10.06 (s, 1H; CHO), 7.94−7.89 (m, 4H; H_{Ar}), 6.28 (s, 1H; NH), 3.48−3.43 (m, 2H; $NHCH_2$), 1.66−1.59 (m, 2H; CH_2), 1.34−1.26 (m, 14H; 7 CH_2), 0.087 (t, J = 6.8 Hz, 3H; CH_3); HRMS: (ESI^+) m/z 290.2125 (observed), 290.2115 (calcd for $[M + H]^+$).

*4-Formyl-N-tetradecylbenzamide (**11d**).* Yield 75%; ^1H NMR (400 MHz, $CDCl_3$) δ/ppm: 10.07 (s, 1H; CHO), 7.90 (s, 4H; H_{Ar}), 6.24 (s, 1H; NH), 3.49−3.44 (m, 2H; $NHCH_2$), 1.62 (d, J = 7.2 Hz, 2H; CH_2), 1.25 (bs, 22H; $11CH_{2(C14\ alkyl\ chain)}$), 0.087 (t, J = 7.2 Hz, 3H; CH_3); HRMS: (ESI^+) m/z: 346.2734 (observed), 346.2741 (calcd for $[M + H]^+$).

*General Protocol for the Synthesis of Aryl−Alkyl Vancomycins (AAVs, **1**−**12**).* A solution of vancomycin (0.050 g, 0.033 mmol, 1 equiv) in DMF (1 mL) and DMSO (1 mL) and DIPEA (12 μL, 5.0 equiv) mixture was maintained at 50 °C. The respective aldehydes (**1a**−**11a** and 4-chlorobiphenyl-carboxaldehyde) were added (0.083 mmol, 2.5 equiv) keeping the reaction in an oil bath, and the reaction was continued at 50 °C for 2 h. After cooling, $NaCNBH_3$ (0.017 mmol, 5.0 equiv) in MeOH was added, and the reaction mixture was allowed to stir at 50 °C for another 2 h after which the reaction was allowed to continue for 20 h. Pure products were isolated by purification using preparative RP-HPLC (gradient: 5−95% acetonitrile/water, 20 min) to more than 95% purity. The product was lyophilized to afford white solid powder bis-trifluoroacetate salts (**1**−**3** and **12**) and tris-trifluoroacetate salts (**4**−**11**).

*AAV-C8 (**1**).* Yield 51%; HPLC purity 96%, ^1H NMR(DMSO-d_6, 400 MHz, 298 K) δ/ppm: 9.45 (s, 1H), 9.17−9.08 (m, 1H), 9.08 (s, 1H), 8.68 (s, 1H), 8.56−8.44 (m, 2H), 8.29 (br, 1H), 7.87−7.85 (m, 3H), 7.63 (s, 1H), 7.54 (d, J = 8.0 Hz, 3H), 7.51−7.41 (m, 3H), 7.37−7.13 (m, 5H), 7.08−7.01 (m, 1H), 6.82−6.75 (m, 1H), 6.75−6.67 (m, 2H), 6.62−6.53 (m, 2H), 6.40 (s, 1H), 6.25 (s, 1H), 6.01−5.89 (m, 2H), 5.83−5.69 (m, 2H), 5.65−5.50 (m, 2H), 5.44−5.33 (m, 2H), 5.29 (s, 1H), 5.23−5.16 (m, 2H), 5.15−5.08 (m, 1H), 4.99−4.88 (m, 1H), 4.73−4.64 (m, 1H), 4.5−4.39 (m, 2H), 4.29−4.16 (m, 1H), 4.08−4.0 (s, 1H), 3.76−3.63 (m, 3H), 3.61−3.56 (m, 1H), 3.48−3.42 (bs, 2H), 3.24 (d, J = 6.4 Hz, 3H), 2.75−2.66 (m, 1H), 2.39−2.27 (m, 2H), 2.17−2.08 (m, 2H), 1.89−1.79 (m, 1H), 1.71−1.59 (m, 2H), 1.55−1.42 (m, 5H), 1.28−1.25 (m, 12H), 1.13 (d, J = 6.0 Hz, 3H), 0.92−0.84 (m, 9H). HRMS: (ESI^+) 848.3051 (observed), 848.3099 (calcd for $[M + 2H]^{2+}$).

*AAV-C10 (**2**).* Yield 55%; HPLC purity 95%; ^1H NMR (DMSO-d_6, 400 MHz, 298 K) δ/ppm: 9.45 (bs, 1H), 9.17 (s, 1H), 9.10 (s, 1H), 9.03−8.90 (m, 1H), 8.68 (s, 1H), 8.58−8.47 (m, 2H), 8.24 (bs, 1H), 7.92−7.84 (m, 3H), 7.63−7.56 (m, 3H), 7.52−7.43 (m, 2H), 7.37−7.32 (m, 1H), 7.22 (d, J = 8.0 Hz, 1H), 7.17 (s, 1H), 7.09−7.01 (m, 1H), 6.81−6.65 (m, 3H), 6.41 (s, 1H), 6.25 (s, 1H), 5.99 (bs, 2H), 5.85−5.73 (m, 2H), 5.62 (s, 1H), 5.41−5.28 (m, 2H), 5.26−5.12 (m, 3H), 4.93−4.90 (m, 1H), 4.68 (d, J = 6.0 Hz, 1H), 4.43 (d, J = 5.6 Hz, 2H), 4.31−4.17 (m, 2H), 4.15−4.02 (m, 2H), 3.96 (bs, 1H), 3.76−3.67 (m, 1H), 3.48 (m, 2H), 3.30−3.23 (m, 5H), 2.64 (m, 2H), 2.54 (s, 1H), 2.20−2.07 (m, 1H), 1.91−1.81 (m, 1H), 1.74−1.67 (m, 1H), 1.65−1.58 (m, 2H), 1.51 (bs, 4H), 1.24 (bs, 15H), 1.15−1.11 (d, J = 8.0 Hz, 3H), 0.95−0.8 (m, 9H). HRMS: (ESI^+) 862.3278 (observed), 862.3246 (calcd for $[M + 2H]^{2+}$).

*AAV-C14 (**3**).* Yield 52%; HPLC purity 96%; ^1H NMR (DMSO-d_6, 400 MHz, 298 K) δ/ppm: 9.44 (s, 1H), 9.17−9.08 (m, 2H), 8.68 (s, 1H), 8.53−8.47 (m, 2H), 8.24 (bs, 1H), 7.88−7.85 (m, 3H),7.58−7.40 (m, 2H), 7.33 (d, J = 8.4 Hz, 1H), 7.23 (d, J = 8.0 Hz, 1H), 7.18 (s, 1H), 7.01 (bs, 1H), 6.80−6.66 (m, 3H), 6.40 (s, 1H), 6.25 (s, 1H), 5.98−5.94 (m, 2H), 5.76 (d, J = 7.6 Hz, 2H), 5.62 (s, 1H), 5.40−5.27 (m, 3H), 5.19 (s, 2H), 5.12 (s, 2H), 4.93−4.92 (bs, 1H), 4.69 (d, J = 6.4 Hz, 1H), 4.5−4.39 (m, 2H), 4.33−4.16 (m, 2H), 4.13−3.96 (m, 3H), 3.78−3.52 (m, 4H), 3.46 (s, 2H), 3.24 (d, J = 6.0 Hz, 2H), 2.60−2.54 (m, 8H), 2.20−2.06 (m, 2H), 2.19−2.06 (m, 2H), 1.85−1.81 (m, 1H), 1.69−1.59 (m, 1H), 1.55−1.43 (m, 4H), 1.24 (bs, 15H), 1.13 (d, J = 6.0 Hz, 3H), 0.95−0.8 (m, 9H). HRMS: (ESI^+) 890.3647 (observed), 890.3617 (calcd for $[M + 2H]^{2+}$).

*AAV-qC6 (**4**).* Yield 60%; HPLC purity 96%; ^1H NMR (DMSO-d_6, 400 MHz, 298 K) δ/ppm: 9.43 (s, 1H), 9.16 (s, 1H), 9.08 (s, 1H), 8.67 (s, 2H), 8.53 (s, 2H), 7.88−7.85 (m, 3H), 7.58−7.51 (m, 3H), 7.49−7.44 (m, 2H), 7.32 (d, J = 8.4 Hz, 1H), 7.25 (d, J = 8.4 Hz, 1H), 7.18 (s, 1H), 6.98 (bs, 1H), 6.79−6.77 (m, 1H), 6.72−6.68 (m, 2H), 6.54 (s, 1H), 6.39 (s. 1H), 6.25 (s, 1H), 5.95 (d, J = 6.4 Hz, 2H), 5.86 (bs, 1H), 5.75 (s, 2H), 5.60 (s, 1H), 5.37 (d, J = 7.6 Hz, 1H), 5.35−5.25 (m, 2H), 5.19 (m, 2H), 5.12−5.10 (m, 2H), 4.91 (s, 1H), 4.68 (d, J = 6.4 Hz, 1H), 4.48−4.43 (m, 2H), 4.29 (s, 1H), 4.20 (d, J = 11.6 Hz, 1H), 4.08 (t, J = 5.2 Hz, 1H), 4.03 (s, 3H), 3.74−3.66 (m, 1H), 3.62−3.58 (m, 1H), 3.57−3.49 (m, 3H), 3.18 (s, 6H), 3.06 (q, J = 6.4 Hz, 2H), 2.55−2.54 (m, 1H), 2.33−2.32 (m, 1H), 2.19−2.10 (m, 1H), 2.01−1.91 (m, 2H), 1.83 (d, J = 10.4 Hz, 1H), 1.72−1.64 (m, 1H), 1.43−1.35 (m, 2H), 1.39 (t, J = 6.8 Hz, 2H), 1.23 (bs, 6H), 1.13 (d, J = 6.0 Hz, 3H), 0.92−0.83 (m, 9H). HRMS: (ESI^+) 905.3505 (observed), 905.3496 (calcd for $[M + H]^{2+}$).

https://doi.org/10.1021/acs.jmedchem.1c00449
J. Med. Chem. 2021, 64, 10185−10202

*AAV-qC8 (**5**).* Yield 40%; HPLC purity 95%; ^{1}H NMR (DMSO-d_6, 400 MHz, 298 K) δ/ppm: 9.42 (s, 1H), 9.15 (s, 1H), 9.07 (s, 1H), 8.65 (bs, 2H), 8.53−8.46 (m, 2H), 7.85 (s, 3H), 7.58−7.51 (m, 2H), 7.48−7.42 (m, 2H), 7.31 (d, J = 8.4 Hz, 1H), 7.26 (d, J = 7.6 Hz, 1H), 7.18 (s, 1H), 6.96 (bs, 1H), 6.81−6.78 (m, 1H), 6.73−6.68 (m, 2H), 6.58 (bs, 1H), 6.39 (m. 1H), 6.23 (m, 1H), 5.95 (d, J = 6.8 Hz, 1H), 5.82 (bs, 1H), 5.78−5.76 (m, 2H), 5.6 (s, 1H), 5.37 (d, J = 7.6 Hz, 1H), 5.30 (bs, 2H), 5.21−5.15 (m, 2H), 5.11−5.09 (m, 2H), 4.89 (bs, 1H), 4.68 (d, J = 6.4 Hz, 1H), 4.49−4.41 (m, 2H), 4.30 (s, 1H), 4.20 (d, J = 11.2 Hz, 1H), 4.10−4.02 (m, 1H), 4.02 (s, 2H), 3.72−3.68 (m, 1H), 3.6−3.43 (m, 4H), 3.18 (s, 6H), 3.06 (q, J = 6.8 Hz, 3H), 2.33−2.32 (m, 1H), 2.20−2.08 (m, 2H), 1.96 (t, J = 8.0 Hz, 3H), 1.82−1.81 (m, 1H), 1.73−1.66 (m, 1H), 1.54−1.44 (m, 3H), 1.39 (t, J = 6.4 Hz, 2H), 1.24 (bs, 10H), 1.13 (d, J = 5.2 Hz, 3H), 0.92−0.84 (m, 9H). HRMS: (ESI$^+$) 919.3680 (observed), 919.3700 (calced for [M + H]^2).

*AAV-qC10 (**6**).* Yield 42%; HPLC purity 98%; ^{1}H NMR (DMSO-d_6, 400 MHz, 298 K) δ/ppm: 9.44 (br, 1H), 9.16 (s, 1H), 9.07 (s, 1H), 8.81 (bs, 1H), 8.70 (bs, 2H), 8.59−8.49 (m, 2H), 8.27 (bs, 1H), 7.91−7.83 (m, 3H), 7.61−7.54 (m, 3H), 7.51−7.46 (m, 3H), 7.33 (d, J = 8.4 Hz, 1H), 7.22−7.17 (m, 2H), 7.05 (s, 1H), 6.80−6.76 (m, 1H), 6.72−6.68 (m, 2H), 6.55−6.53 (m, 1H), 6.25 (s, 1H), 6.00−5.94 (m, 2H), 5.84 (bs, 1H), 5.68 (d, J = 8.0 Hz, 1H), 5.63 (s, 1H), 5.38−5.33 (d, 2H), 5.31 (s, 1H), 5.22−5.16 (m, 2H), 5.12−5.10 (m, 2H), 4.93 (bs, 1H), 4.69 (d, J = 6.4 Hz, 1H), 4.49−4.41 (m, 2H), 4.28−4.16 (m, 2H), 4.13−4.01 (m, 5H), 3.95 (bs, 1H), 3.7 (m, 1H), 3.62−3.49 (m, 4H), 3.18 (s, 6H), 3.07 (d, J = 6.4 Hz, 2H), 2.63 (bs, 3H), 2.55 (s, 1H), 2.33−2.32 (m, 1H), 2.21−2.08 (m, 2H), 2.00−1.95 (m, 2H), 1.88−1.80 (m, 1H), 1.73−1.55 (m, 3H), 1.49 (s, 2H), 1.40 (t, J = 6.0 Hz, 2H), 1.24 (bs, 15H), 1.13 (d, J = 6.0 Hz, 3H), 0.91 (d, J = 5.6 Hz, 3H), 0.88−0.83 (m, 6H). HRMS: (ESI$^+$) 933.3817 (observed), 933.3825 (calcd for [M + H]$^{2+}$).

*AAV-qC12 (**7**).* Yield 43%; HPLC purity 98%; ^{1}H NMR (DMSO-d_6, 400 MHz, 298 K) δ/ppm: 9.44 (bs, 1H), 9.16 (s, 1H), 9.07 (s, 1H), 8.69 (s, 1H), 8.57−8.48 (m, 2H), 8.25 (br, 2H), 7.9−7.82 (m, 3H), 7.6−7.53 (m, 3H), 7.51−7.42 (m, 3H), 7.32 (d, J = 8.4 Hz, 1H), 7.23 (d, J = 8.4 Hz, 1H), 7.18 (s, 1H), 7.01 (bs, 1H), 6.82−6.77 (m, 1H), 6.73−6.67 (m, 1H), 6.55 (s, 1H), 6.39 (bs, 1H), 6.24 (s, 1H), 5.99−5.91 (m, 2H), 5.83 (bs, 1H), 5.76 (d, J = 7.6 Hz, 1H), 5.62 (s, 1H), 5.4−5.28 (m, 3H), 5.19 (s, 2H), 5.12 (s, 2H), 4.93−4.92 (m, 1H), 4.72−4.65 (m, 1H), 4.49−4.41 (m, 2H), 4.29−4.16 (m, 2H), 4.13−3.99 (m, 4H), 3.74−3.66 (m, 1H), 3.59−3.50 (m, 5H), 3.18 (s, 6H), 3.07 (q, J = 6.4 Hz, 2H), 2.57 (m, 2H), 2.34−2.31 (m, 1H), 2.17−2.07 (m, 2H), 2.0−1.95 (m, 2H), 1.88−1.79 (m, 1H), 1.7−1.6 (m, 2H), 1.53−1.45 (m, 2H),1.43−1.36 (m,2H) 1.24 (br,18H), 1.13 (d, J = 6.0 Hz, 3H), 0.92−0.83 (m, 9H). HRMS: (ESI$^+$) 947.3984 (observed), 947.3965 (calcd for [M + H]$^{2+}$).

*AAV-qC14 (**8**).* Yield 45%; HPLC purity 99; ^{1}H NMR (DMSO-d_6, 400 MHz, 298 K) δ/ppm: 9.44 (bs, 1H), 9.16 (s, 1H), 9.08 (s, 1H), 8.69 (s, 1H), 8.54 (t, J = 5.6 Hz, 2H), 8.25 (bs, 2H), 7.89−7.84 (m, 3H), 7.59−7.52 (m, 3H), 7.50−7.41 (m, 2H), 7.32 (d, J = 8.4 Hz, 1H), 7.24 (d, J = 8.4 Hz, 2H), 7.18 (s, 1H), 7.00 (s, 1H), 6.79−6.77 (m, 1H), 6.73−6.68 (m, 2H), 6.55 (s, 1H), 6.39 (s, 1H), 6.25 (s, 1H), 5.95 (d, J = 6.4 Hz, 1H), 5.91 (s, 1H), 5.76 (d, J = 8.0 Hz, 1H), 5.61 (s, 1H), 5.41−5.27 (m, 3H), 5.19 (s, 2H), 5.11 (s, 2H), 4.92 (bs, 1H), 4.73−4.64 (m, 1H), 4.49−4.41 (m, 2H), 4.32−4.17 (m, 2H), 4.11−4.09 (m, 1H), 4.03 (s, 3H), 3.75−3.65 (m, 1H), 3.59−3.44 (m, 3H), 3.18 (s, 6H), 3.07 (q, J = 6.4 Hz, 2H), 2.54 (m, 2H), 2.34−2.31 (m, 1H), 2.19−2.07 (m, 2H), 1.99−1.92 (m, 2H), 1.87−1.79 (m, 1H), 1.70−1.59 (m, 2H), 1.48 (s, 2H), 1.40 (s, 2H), 1.24 (bs, 22H), 1.13 (d, J = 6.0 Hz, 3H), 0.93−0.80 (m, 9H). HRMS: (ESI$^+$) 961.4145 (observed), 961.4122 (calcd for [M$^+$ + H]$^{2+}$).

*AAV-qPh (**9**).* Yield 44%; HPLC purity 94%; ^{1}H NMR (DMSO-d_6, 400 MHz, 298 K) δ/ppm: 9.43 (s, 1H), 9.17 (s, 1H), 9.06 (s, 1H), 8.73−8.47 (m, 3H), 8.17 (bs, 2H), 7.86 (s, 1H), 7.57−7.42 (m, 8H), 7.33 (d, J = 8.0 Hz, 1H), 7.23 (d, J = 8.0 Hz, 1H), 7.17 (s, 1H), 7.05 (s, 1H), 6.80−6.68 (m, 2H), 6.53 (m, 1H), 6.39 (d, 1H), 6.25 (s, 1H), 5.97 (d, J = 6.4 Hz, 1H) 5.90 (s, 1H), 5.79−5.75 (m, 1H), 5.63 (s, 1H), 5.37−5.30 (m, 2H), 5.18−5.10 (m, 3H), 4.92 (bs, 1H), 4.68 (d, J = 6.0 Hz, 1H), 4.44−4.42 (m, 2H),4.29−4.16 (m, 1H), 4.10 (t, J = 5.2 Hz, 1H), 4.04−3.96 (m, 2H), 3.75−3.66 (m, 1H), 3.62−3.50 (m, 2H),3.49−3.43 (m, 2H), 2.99 (s, 1H), 2.91−2.83 (m, 1H), 2.67 (s, 2H), 2.55 (s, 6H), 2.33 (s, 1H), 2.19−2.06 (m, 2H), 1.83−1.80 (m, 1H), 1.71−1.59 (bs, 2H), 1.51−1.47 (bs, 4H), 1.24 (bs, 2H), 1.13 (d, J = 5.6 Hz, 3H), 0.89 (dd, J = 18.8 Hz, 5.6 Hz, 6H). HRMS: (ESI$^+$) 879.8193 (observed), 879.8154 (calcd for [M$^+$ + H]$^{2+}$).

*AAV-qNaph (**10**).* Yield 46%; HPLC purity 92%; ^{1}H NMR (DMSO-d_6, 400 MHz, 298 K) δ/ppm: 9.45 (s, 1H), 8.70−8.64 (m, 2H), 8.50−8.47 (m, 2H), 8.12 (d, J = 8.0 Hz, 1H), 8.05 (d, J = 8.0 Hz, 1H), 7.88−7.84 (m, 2H), 7.80 (d, J = 7.2 Hz, 1H), 7.69−7.53 (m, 6H), 7.5−7.41 (m, 1H), 7.44−7.36 (m, 2H), 7.32 (d, J = 8.0 Hz, 1H), 7.26 (d, J = 8.0 Hz, 1H), 7.19 (s, 1H), 6.94 (s, 1H), 6.79−6.77 (m, 1H), 6.73−6.69 (m, 2H), 6.61 (s, 1H), 6.4 (s, 1H), 6.25 (s, 1H), 5.95 (d, J = 5.6 Hz, 2H), 5.86 (s, 1H), 5.75 (d, J = 7.6 Hz, 1H), 5.59 (s, 1H), 5.39−5.33 (m, 2H), 5.28 (s, 1H), 5.22−5.12 (m, 2H), 5.06 (s, 2H), 4.69 (d, J = 6.4 Hz, 1H), 4.44−4.42 (m, 2H), 4.22−4.20 (m, 1H), 4.09−4.08 (m, 1H), 3.97 (bs, 1H), 3.71−3.69 (m, 1H), 3.56−3.49 (m, 4H), 3.00 (s, 6H), 2.44 (s, 3H), 2.19−2.08 (m, 4H), 1.87−1.79 (m, 1H), 1.7−1.59 (m, 2H),1.51−1.37 (m, 3H), 1.14−1.12 (m, 3H), 0.88 (dd, J = 18.4 Hz, 6.4 Hz, 6H). HRMS: (ESI$^+$) 904.8256 (observed), 904.8280 (calcd for [M$^+$+H]$^{2+}$).

*AAV-qBiph (**11**).* Yield 42%; HPLC purity 96%; ^{1}H NMR (DMSO-d_6, 400 MHz, 298 K) δ/ppm: 9.45 (s, 1H), 9.17 (s, 1H), 9.09 (s, 1H), 8.75 (bs, 1H), 8.68 (s, 2H), 8.52−8.51 (m, 1H), 7.89 (t, J = 8.0 Hz, 2H), 7.73−7.59 (m, 6H), 7.55 (d, J = 6.0 Hz, 3H), 7.51−7.47 (m, 4H), 7.44−7.38 (m, 1H), 7.34 (d, J = 6.0 Hz, 1H), 7.23 (d, J = 8.4 Hz 2H), 7.18 (bs, 1H), 7.02 (bs, 1H), 6.78 (d, J = 8.4 Hz, 1H), 6.73−6.69 (m, 2H), 6.57 (s, 1H), 6.4 (s, 1H), 6.25 (s, 1H), 5.98−5.96 (m, 2H), 5.70 (d, J = 7.6 Hz 1H), 5.62 (s, 1H), 5.37−5.35 (m, 2H), 5.30 (s, 1H), 5.19 (s, 2H), 4.93 (bs, 1H), 4.70 (d, J = 6.4 Hz, 1H), 4.47 4.43 (m, 2H), 4.28−4.19 (m, 2H), 4.09 (t, J = 5.2 Hz, 1H), 4.04−4.00 (m, 1H), 3.77−3.70 (m, 1H), 3.72−3.69 (m, 2H), 3.63−3.45 (m, 3H), 3.01 (s, 6H), 2.57 (s, 2H), 2.19−2.07 (m, 4H),1.84 (d, J = 12.0 Hz, 1H), 1.71−1.64 (m, 2H), 1.53−1.43 (m,3H), 1.14 (d, J = 6.4 Hz, 3H), 0.88 (dd, J = 19.6 Hz,6.0 Hz 6H). HRMS: (ESI$^+$) 917.8320 (observed), 917.8310 (calcd for [M + H]$^{2+}$).

*CBP-Van (**12**).* Yield 45%; HPLC purity 95%; ^{1}H NMR (DMSO-d_6, 400 MHz, 298 K) δ/ppm: 9.45 (s, 1H), 8.58 (bs, 1H), 8.43−8.21 (m, 1H), 8.05−7.79 (m, 2H), 7.78−7.56 (m, 5H), 7.55−7.43 (m, 4H), 7.43−7.19 (m, 3H), 6.89−6.64 (m, 2H), 6.36 (d, J = 14.8 Hz, 1H), 5.87−5.70 (m, 1H), 5.55−5.52 (m, 1H), 5.42−5.12 (m, 4H), 4.94−4.68 (m, 2H), 4.61−4.36 (m, 2H), 4.33 (d, 1H), 4,.17 (bs, 1H), 4.00 (bs, 2H), 3.85 (d, J = 13.2 Hz, 1H), 3.73−3.62 (m, 1H), 3.6−3.51 (m, 2H), 3.12 (s, 1H), 3.03−2.98 (m, 1H), 2.54 (s, 2H), 2.33−2.16 (m, 2H),1.77−1.56 (m, 2H), 1.28−1.19 (bs, 2H), 1.1−1.01 (m, 3H), 0.99−0.82 (m, 6H). HRMS ESI$^+$$m/z$: 825.7471 (observed), 825.7454 (calcd for [M + 2H]$^{2+}$).

*Protocol for the Synthesis of Control Compound **13**.* p-Toluic acid (1 equiv) and DIPEA (5.0 equiv) were dissolved in a 4:1 mixture of DCM/DMF. The reaction mixture was cooled to 4 °C and HBTU (1.2 equiv) was added. Compound **3c** (1.1 equiv) was then added to the reaction mixture and allowed to stir for 24 h at room temperature. Following this, the reaction mixture was diluted with DCM and was washed sequentially with water, 1 N HCl solution, and aqueous saturated bicarbonate solution. The organic layer was dried over anhydrous sodium sulfate, filtered, and concentrated in vacuo. A pure product was obtained through column chromatography using silica as the stationary phase (gradient: 60%−70% ethyl acetate/hexane).

*N-(2-(Decylamino)-2-oxoethyl)-N,N-dimethyl-3-(4-methylbenzamido)propan-1-aminium Trifluoroacetate (**13**).* Yield 65%; ^{1}H NMR (DMSO-d_6, 400 MHz, 298 K) δ/ppm: 8.53 (s, 1H; NH), 8.46 (s, 1H; NH), 7.74 (d, J = 6.8 Hz, 1H; Ar_H), 7.27 (s, 2H; H_{Ar}), 4.00 (s, 2H; COCH_2NMe$_2^+$), 3.56−3.52 (m, 2H; CH_2NMe$_2^+$), 3.18 (s, 6H; N$^+$(CH_3)$_2$), 3.07−3.04 (m, 2H; CH_2CH$_2$NHCO), 2.35 (s, 3H; PhCH_3), 1.96−1.94 (m, 2H; CH_2NH), 1.38−1.36 (m, 2H; CH_2CH$_2$CH$_2$NHCO), 1.23 (s, 16H; C$H_{2(\text{alkyl chain})}$), 0.86−0.84 (m,3H; C$H_3$); HRMS ESI$^+$ m/z: 418.3434 (observed), 418.3429 (calcd for M$^+$).

Biological Assays. *Antibacterial Assay.* The antibacterial activities of the compounds are reported as their MIC, which is the

https://doi.org/10.1021/acs.jmedchem.1c00449
J. Med. Chem. 2021, 64, 10185−10202

lowest concentration of the antibacterial agent required to inhibit the growth of microorganism after overnight incubation. All synthesized compounds (**1**−**12**) were assayed in a microdilution broth format as per the CLSI guideline. 5 μL of the frozen bacterial stock was added to 3 mL of the respective broth and cultured for 6 h at 37 °C prior to the experiments. This 6 h grown culture gives about 10^9 cfu/mL, which was determined by the spread plating method. This was then diluted to a cell concentration of 10^5 cfu/mL, which was then used for MIC determination. The test compounds were serially diluted 2-fold, in sterile millipore water and 50 μL of the serial dilutions were added to the wells of a 96-well plate, followed by the addition of 150 μL of the bacterial solution. The plates were then incubated for 18−24 h at 37 °C. The O.D. value at 600 nm was recorded using a TECAN (Infinite series, M200 pro) Plate Reader. Each concentration had triplicate values and repeated at least twice, and the MIC value was determined by taking the average concentration for no visual turbidity and OD_{600} values.

Hemolysis Assay. The assay was performed as described in our previously published protocols.[43] Freshly drawn, heparinized human blood was centrifuged down to obtain the erythrocytes and resuspended to 5 vol % in PBS (pH 7.4). 150 μL of the erythrocyte suspension was added to 50 μL of serially diluted compounds taken in 96-well microtiter plates. One column without compound and other with 50 μL of 1 vol % solution of Triton X-100 were kept as negative and positive controls, respectively. The plates were incubated at 37 °C for 1 h, followed by centrifugation at 3500 rpm for 5 min 100 μL of the supernatant from each well were transferred into fresh microtiter plates, and A_{540} was measured.

Percentage of hemolysis was determined using the formula $(A - A_0)/(A_{total} - A_0) \times 100$, where A is the absorbance of the test well, A_0 is the absorbance of the negative controls (without compound), and A_{total} is the absorbance of 100% hemolysis wells (with Triton X-100), all measured at 540 nm.

AlamarBlue Assay (Cytotoxicity Assay). The standard protocol as mentioned in the kit was followed. Briefly, 2×10^4 HEK 293cells were seeded per well in 100 μL of Dulbecco's modified Eagle's medium (DMEM) in a 96-well plate and incubated for 24 h. Compounds were treated at various concentrations and incubated for 24 h after which 10 μL of 10 × Alamar blue dye was added. 2 h postincubation with the dye, the absorbance was measured at 570 nm using 600 nm as the reference wavelength.

Fluorescence Microscopy of HEK Cells. Approximately 10^4 HEK 293 cells were seeded into each well of a 96-well plate overnight under a 5% CO_2 atmosphere at 37 °C. 100 μL of30 μM solution of AAV-qC10 in DMEM medium was added to the seeded cells and incubated for 24 h. One row of cells was treated with 0.1% Triton-X and one row was left untreated as positive and negative controls, respectively. Postincubation, cells were washed with 1× PBS and then stained with 50 μL of 1:1 calcein AM (2 μM) and PI (4.5 μM) for 15 min under a 5% CO_2 atmosphere at 37 °C. The excess dye was then removed by washing the cells with 1×PBS, and images were captured with a 40× objective of a Leica DM2500 fluorescence microscope. For imaging, a band-pass filter for Calcein AM (at 500−550 nm) and a long-pass filter for PI (at 590−800 nm) were used.

Time-Kill Kinetics Assay. The bactericidal activity of the compounds was evaluated with the time kill kinetics assay according to the previously published protocol.[44] Briefly, MRSA and VRE were, respectively, cultured in nutrient and BHI broth at 37 °C for 6 h. AAV-qC10and vancomycin were added individually to the bacterial solution (approximately 6.1 log cfu/mL of MRSA and 5 log cfu/mL of VRE ATCC 51575) at MIC, 2 × MIC, and 4 × MIC. This was then incubated at 37 °C and at different time intervals (0, 2, 4, 6, and 24 h), and 20 μL of aliquots were taken out and serially diluted 10-fold in 0.9% saline. 20 μL of the solutions were then plated on nutrient agar plates and incubated at 37 °C for 24 h. The viable bacterial colonies were counted and the results are represented on a logarithmic scale, that is, log cfu/mL.

Antagonization Assays. Antagonization of antibacterial activity of AAV-qC10 was determined by adding 500μM *N,N′*-diacetyl-L-Lys-D-Ala-D-Ala or 100 μg/mL of lipoteichoic acid to serial dilutions of the test compound and preincubating for 10 min and 1 h, respectively. The MIC was then determined against MRSA by measuring the OD_{600} 18−24 h postincubation.

Membrane Permeabilization Assay. Midlog phase cultures of *B. subtilis*, VRE, and MRSA were harvested (3500 rpm, 5 min), washed, and resuspended in a 1:1 solution of 5 mM glucose and 5 mM HEPES buffer (pH 7.2).[45,46] 10 μM of PI was added to the bacterial suspension and 180 μL of this mixture was put into 96-well flat clear bottomed black well plates. Fluorescence was monitored at an excitation wavelength of 535 nm (slit width: 10 nm) and an emission wavelength of 617 nm (slit width: 5 nm). After this, 20 μL of test compounds at 10 μM were added to the wells containing bacterial suspension. The uptake of PI was monitored by the increase in fluorescence for 30−40 min as a measure of membrane permeabilization. Mid-log phase cells were treated with vancomycin and AAV-qC10 at 10 μM, respectively. For membrane permeabilization against stationary phase and persister cells of MRSA, compounds vancomycin and AAV-qC10 were treated at 20 μM, respectively.

Cytoplasmic Membrane Depolarization Assay. Mid-log phase cultures of *B. subtilis*, MRSA, and VRE were harvested (3500 rpm, 5 min), washed in 1:1 solution of 5 mM glucose and 5 mM HEPES buffer (pH 7.2), and resuspended in 1:1:1 solution of 5 mM HEPES buffer, 5 mM glucose, and 100 mM KCl solution.[44,46] 2 μM of 3,3′-Dipropylthiadicarbocyanine iodide ($DiSC_3(5)$) was then added to the bacterial suspension and preincubated for 20−30 min. The fluorescence was monitored at an excitation wavelength of 622 nm (slit width: 10 nm) and an emission wavelength of 670 nm (slit width: 5 nm). Then, 20 μL of test compounds were added to polystyrene-black well microplates containing bacterial suspension and $DiSC_3(5)$ after 2−4 min of fluorescence measurement. The fluorescence was monitored for another 35−40 min as a measure of membrane depolarization. To assess for interference of AAV-qC10 and vancomycin with the fluorescence of $DiSC_3(5)$, 10 μM of the test compounds were individually incubated with 2 μM solution of $DiSC_3(5)$ and the fluorescence of $DiSC_3(5)$ was monitored at 2 min intervals. The fluorescence was then measured at the above mentioned wavelengths. A decrease in the fluorescence intensity possibly results due to the interaction of the dye with the polystyrene-surface of the 96-well microtiter plate.[47] Mid-log phase cells were treated with vancomycin and AAV-qC10 at 10 μM, respectively. For membrane depolarization against stationary phase and persister cells of MRSA, compounds vancomycin and AAV-qC10 were treated at 20 μM, respectively.

Determination of MIC against *B. subtilis*. An inoculum of *B. subtilis* 168 was cultured overnight in 5 mL BMM medium at 37 °C to the mid-log phase. BMM medium consists of 50 mM Tris, 15 mM $NH_4(SO_4)_2$, 8 mMMgSO_4, 27 mMKC1, 7 mM sodium citrate, 0.1% glucose, 0.6 mMKH_2PO_4, and 16 μg/mL of L-tryptophan and glutamic acid.[48] The bacteria in the mid-log phase were then diluted to an OD_{500} of 0.005 (yielding a final concentration of 5×10^5 cells/ml) and incubated with serial dilutions of the compound for 18 h at 37 °C in BMM medium. The MIC was determined as the lowest concentration at which no visible turbidity was observed.

Determination of Physiologically Effective Concentration. *B. subtilis* 168 was grown overnight in 50 mL flasks with 10 mL of BMM medium. Upon reaching the mid-log phase (an OD_{500} between 0.5 and 1), an inoculum was grown in 100 mL of BMM in a 500 ml flask. When OD_{500} of the cultures reached 0.35, 5 mL of the bacterial culture was aliquoted out into separate conical tubes and test compounds were added. The OD_{500} of the aliquots was recorded every 30 min[27] The concentration that retards the growth of exponentially growing bacteria was defined as the PEC.

Cell Wall Biosynthesis Inhibition Assay or Bubble Assay. Overnight cultures of *B. subtilis* 168 in the mid-log phase were diluted in BMM and allowed to grow to an OD_{500} of 0.35.200 μL of the bacterial culture were treated with the required concentrations of test compounds at PEC for 15 min at 37 °C. The cells were then fixed with 1 mL of a 1:3 mixture of acetic acid/methanol.[27] The morphology of the bacterial cells was examined through a light microscope.

https://doi.org/10.1021/acs.jmedchem.1c00449
J. Med. Chem. 2021, 64, 10185−10202

GFP-MinD Localization. *B. subtilis* 1981 GFP-MinD was cultured overnight in BMM.[28] Cells were then inoculated in xylose containing BMM instead of glucose to an OD_{500} of 0.1 to induce expression of the GFP-MinD fusion protein. Upon reaching an OD_{500} of 0.35, the cells were treated with test compounds at the PEC (vancomycin, AAV-qC10) and 0.75 μg/mL (nisin) for 15 min. 0.5 μL of nonfixed, nonimmobilized samples of the culture was imaged immediately in the fluorescent mode (an Olympus microscope with a U-LH100HGAPOburner and a U-RFL-T power supply).

BAC Light Assay. Overnight cultures of *B. subtilis* 168 were inoculated in BMM and grown to an OD_{500} of 0.35.500 μL of the bacterial culture was then treated with the compounds at required concentrations for 10 min in the same medium at 37 °C. The bacteria were then centrifuged down at 13,200 rpm and resuspended in prewarmed BMM medium. 2 μL of 1:1 BAC light dye was then added to the bacterial suspension and incubated for 5 min. The fluorescence for the respective dyes was observed under a microscope in the GFP and Texas Red channels.

Resistance Study. Vancomycin was chosen as the control antibiotic for MRSA. The initial MIC values of AAV-qC10 and vancomycin were determined against the respective bacteria. The initial MIC of vancomycin was 0.6 μM and that of AAV-qC10 was 0.9 μM. After the initial MIC experiment, serial passaging was initiated by harvesting bacterial cells growing in the sub-MIC concentration of the compounds and was subjected to another MIC assay.[43] Initially, cells exposed to 0.3 μM of vancomycin, and 0.45 μM for AAV-qC10 (**6**), were collected and taken forward for next passage. The bacterial concentration was adjusted to $\sim 10^5$ cfu/mL based on OD_{600}. The process was repeated for 27 passages. The fold of MIC increased for test compounds was plotted against the number of days.

Growth of Mature Biofilms. A mid-log phase culture of MRSA was diluted to a concentration of approximately 10^5 cfu/mL in a nutrient broth supplemented with 1% w/v glucose and 1% w/v NaCl to make the bacterial stock solution. Biofilms of MRSA were then allowed to form on a 18 mm glass cover-slip by incubating the bacterial solution at 37 °C for 24 h.

Cell Viability of Bacteria in Biofilms. Mature biofilms of MRSA were generated as mentioned earlier and then treated with vancomycin and AAV-qC10 respectively at 20 μM each. The biofilms on glass cover slips were carefully removed from the well and washed 24 h post-treatment with the test compounds. They were then treated with 0.1% Trypsin−EDTA solution for 15 min at 37 °C. Aliquots of the digested biofilms were then serially diluted 10-fold and spot plated on agar plates. The number of viable colonies was counted after 24 h.

Confocal Laser Scanning Microscopy. Glass cover slips 24 h post-treatment with the test compounds and the untreated control were carefully removed from the well, washed, and placed on glass slides. The biofilms were then stained with 10 μL of SYTO9 (60 μM) and imaged using a Zeiss 510 Meta confocal laser-scanning microscope. The orthogonal projections of the images were processed with a LSM 5 Image examiner.

Kinetics of Antibacterial Activity against Metabolically Inactive Bacterial Cells. Bacterial stock of MRSA ATCC33591 was inoculated in nutrient medium and cultured to the mid-log phase at 37 °C. The bacterial suspension was diluted 1000-fold in nutrient media and allowed to reach the stationary phase in 16 h. The bacterial suspension was diluted and spot-plated in Nutrient agar to determine the bacterial count. Persister cells were then generated by treating the stationary phase culture with 100 μg/mL of ampicillin for 3 h. The stationary phase and persister cells were then washed and diluted to $\sim 10^6$ cfu/mL in 1× PBS and treated with test compounds at the respective concentrations. The bacteria were then incubated with varying concentrations of compounds at 37 °C for up to 24 h. Stationary phase cells were treated with AAV-qC10 at 4.5 μM, 9 μM and 22 μM and with vancomycin at 40 μM. Persister cells were treated with AAV-qC10 at 4.5 μM, 9 μM, with vancomycin at 40 μM and ampicillin at 60 μM. At various time points of 2, 4, 6, and 24 h, post-incubation, 20 μL aliquots of the bacterial suspension was serially diluted 10-fold and spot-plated on nutrient agar. The viable bacteria were then counted after 48 h incubation at 37 °C.

Postantibiotic Effect. MRSA ATCC33591 was grown to the exponential growth phase. To study the PAE, AAV-qC10 and vancomycin were incubated with $\sim 9 \times 10^7$ cfu/mL of exponentially growing phase MRSA at 10× MIC. Treatment was carried out for 1 h in Falcon tubes under shaking conditions at 37 °C. Post-treatment, the bacteria were washed to remove the antibiotic and resuspended in culture media and allowed to grow at 37 °C, and the bacterial titer was determined in each case. Aliquots of bacteria were taken out at intervals of 1 h from untreated, vancomycin and AAV-qC10-treated groups. The bacterial titer was determined by serial dilutions and plating on nutrient agar.

In Vivo Toxicology. Groups of four 6 to 8 week old Balb/c female mice were used to determine the systemic toxicity of AAV-qC10. Each mouse was injected with a 0.2 mL of freshly prepared compound solution at 55.5 mg/kg dose through intravenous (i.v) and intraperitoneal (i.p) injection according to the OECD Animals guidelines. They were directly inspected for adverse effects for 4 h, and general health (breathing, mobility, and reactions) and mortality were observed to understand the tolerability of the administered dose for 14 days thereafter.

In Vivo Acute Toxicity. For the evaluation of acute toxicity, five mice were injected with AAV-qC10 through i.p. at 12 mg/kg in 0.2 mL of sterilized saline. Blood samples were collected after 48 h, and the analysis of biochemical parameters such as alanine aminotransferase, urea nitrogen, and creatinine was performed by RV Scientific, Bangalore. These studies proved that the trimethylammonium cation modification was not associated with any significant acute toxicity.

Stability of Compound in Blood Plasma and Liver Homogenate. To examine the susceptibility of AAV-qC10 toward serum proteases, the antibacterial activity was tested in the presence of 50% of plasma and liver homogenate. Briefly, 250 μL of AAV-qC10 was added into 250 μL of fresh human plasma and incubated at 37 °C. An aliquot of the samples 3 h and 24h postincubation was diluted in 0.9% saline and the antibacterial activity (MIC) was determined against MRSA and VRE by following the same protocol as described above for the antibacterial assay.

In Vivo Activity in the Murine Thigh Infection Model. Groups of four 6 to 8 week old Balb/c specific pathogen-free female mice were used (weight ∼ 22 g) for the experiment. The mice were rendered neutropenic by injecting two intraperitoneal doses of cyclophosphamide, 4 days (150 mg kg^{-1}) and 1 day (100 mg kg^{-1}) before the infection experiment. 50 μL of $\sim 10^6$ cfu/mL bacterial inoculum (MRSA) was injected into the thigh. 1 h postinoculation, animals were treated intraperitoneally twice with 12 h intervals with saline, vancomycin (12 mg kg^{-1}), and a single dose of AAV-qC10 (12 mg kg^{-1}). 24 h post the first treatment, the animals were euthanized (using ether) and the thighs were collected aseptically. The thigh tissue was weighed and homogenized. The dilutions of the homogenate were plated onto agar plates, which were incubated overnight at about 37 °C. The bacterial titer was expressed as log cfu/g of thigh weight and plotted in GraphPad Prism software.

■ ASSOCIATED CONTENT

Supporting Information

The Supporting Information is available free of charge at https://pubs.acs.org/doi/10.1021/acs.jmedchem.1c00449.

Synthesis of control compound **13**; fluorescence microscopy images; kinetics of the effect of vancomycin and AAV-qC10 on fluorescence of the $DisC_3(5)$ dye; membrane depolarization and membrane permeabilization against stationary phase cells and persister cells; stability of AAV-qC10 in mouse plasma and liver homogenate; and characterization of AAV-qC10 (PDF)

Molecular formula strings(CSV)

https://doi.org/10.1021/acs.jmedchem.1c00449
J. Med. Chem. 2021, 64, 10185−10202

AUTHOR INFORMATION

Corresponding Author

Jayanta Haldar − *Antimicrobial Research Laboratory, New Chemistry Unit and School of Advanced Materials, Jawaharlal Nehru Centre for Advanced Scientific Research (JNCASR), Bengaluru 560064 Karnataka, India;* orcid.org/0000-0002-8068-1015; Phone: +91 802208 2565; Email: jayanta@jncasr.ac.in

Authors

Paramita Sarkar − *Antimicrobial Research Laboratory, New Chemistry Unit and School of Advanced Materials, Jawaharlal Nehru Centre for Advanced Scientific Research (JNCASR), Bengaluru 560064 Karnataka, India*

Debajyoti Basak − *Antimicrobial Research Laboratory, New Chemistry Unit and School of Advanced Materials, Jawaharlal Nehru Centre for Advanced Scientific Research (JNCASR), Bengaluru 560064 Karnataka, India*

Riya Mukherjee − *Antimicrobial Research Laboratory, New Chemistry Unit and School of Advanced Materials, Jawaharlal Nehru Centre for Advanced Scientific Research (JNCASR), Bengaluru 560064 Karnataka, India*

Julia E. Bandow − *Applied Microbiology, Faculty of Biology and Biotechnology, Ruhr University Bochum, Bochum 44780, Germany*

Complete contact information is available at: https://pubs.acs.org/10.1021/acs.jmedchem.1c00449

Author Contributions

P.S. designed and planned research, performed synthesis, characterization, in vitro microbiological assays and in vivo infection studies, analyzed data, and wrote the manuscript; D.B. performed synthesis, characterization, manuscript writing, and editing; R.M. performed cytotoxicity testing, in vivo activity studies and manuscript editing; J.E.B. designed experiments for mechanisms of action against *B. subtilis* experimental, manuscript writing, and editing; and J.H. designed and supervised research and wrote the manuscript.

Notes

The authors declare no competing financial interest.

ACKNOWLEDGMENTS

J.H. acknowledges the DST-DAAD bilateral cooperation project (INT/FRG/DAAD/P-15/2018), DST-BRICS multilateral cooperation project (DST/IMRCD/BRICS/PilotCall2/MBLI/2018(G)), and JNCASR for funding. J.E.B. acknowledges funding from the DAAD Program DST 2018 (57389759). We thank Pascal Dietze (RUB) for technical support. D.B. acknowledges the postdoctoral fellowship from the DST-BRICS project and R.M. is grateful to the DBT-Research Associateship Program for the postdoctoral fellowship.

ABBREVIATIONS

HRMS, high-resolution mass spectrometry; MIC, minimum inhibitory concentration; cfu, colony forming units; MRSA, methicillin-resistant *S. aureus* ATCC 33591; VRSA, vancomycin-resistant *S. aureus*; VRE, vancomycin-resistant enterococci; GFP, green fluorescent protein; PEC, physiologically effective concentration; HC_{50}, 50% hemolytic activity; PI, propidium iodide; LD_{50}, dose that is lethal in 50% of test mice.

REFERENCES

(1) https://www.who.int/medicines/publications/WHO-PPL-Short_Summary_25Feb-ET_NM_WHO.pdf. (2017). (accessed 25 August 2020)

(2) Lewis, K. Persister cells and the riddle of biofilm survival. *Biochemistry* **2005**, *70*, 267−274.

(3) Fisher, R. A.; Gollan, B.; Helaine, S. Persistent bacterial infections and persister cells. *Nat. Rev. Microbiol.* **2017**, *15*, 453−464.

(4) Brown, E. D.; Wright, G. D. Antibacterial drug discovery in the resistance era. *Nature* **2016**, *529*, 336−343.

(5) Dhanda, G.; Sarkar, P.; Samaddar, S.; Haldar, J. Battle against vancomycin-resistant bacteria: recent developments in chemical strategies. *J. Med. Chem.* **2019**, *62*, 3184−3205.

(6) Reynolds, P. E. Structure, biochemistry and mechanism of action of glycopeptide antibiotics. *Eur. J. Clin. Microbiol. Infect. Dis.* **1989**, *8*, 943−950.

(7) Zhanel, G. G.; Calic, D.; Schweizer, F.; Zelenitsky, S.; Adam, H.; Lagacé-Wiens, P. R. S.; Rubinstein, E.; Gin, A. S.; Hoban, D. J.; Karlowsky, J. A. New lipoglycopeptides. *Drugs* **2010**, *70*, 859−886.

(8) Zeng, D.; Debabov, D.; Hartsell, T. L.; Cano, R. J.; Adams, S.; Schuyler, J. A.; McMillan, R.; Pace, J. L. Approved glycopeptide antibacterial drugs: mechanism of action and resistance. *Cold Spring Harbor Perspect. Med.* **2016**, *6*, a026989.

(9) Binda, E.; Marinelli, F.; Marcone, G. Old and new glycopeptide antibiotics: action and resistance. *Antibiotics* **2014**, *3*, 572−594.

(10) Silhavy, T. J.; Kahne, D.; Walker, S. The bacterial cell envelope. *Cold Spring Harbor Perspect. Med.* **2010**, *2*, a000414.

(11) Bugg, T. D. H.; Braddick, D.; Dowson, C. G.; Roper, D. I. Bacterial cell wall assembly: still an attractive antibacterial target. *Trends Biotechnol.* **2011**, *29*, 167−173.

(12) Ganz, T. Defensins: antimicrobial peptides of innate immunity. *Nat. Rev. Immunol.* **2003**, *3*, 710−720.

(13) Blaskovich, M. A. T.; Hansford, K. A.; Gong, Y.; Butler, M. S.; Muldoon, C.; Huang, J. X.; Ramu, S.; Silva, A. B.; Cheng, M.; Kavanagh, A. M.; Ziora, Z.; Premraj, R.; Lindahl, F.; Bradford, T. A.; Lee, J. C.; Karoli, T.; Pelingon, R.; Edwards, D. J.; Amado, M.; Elliott, A. G.; Phetsang, W.; Daud, N. H.; Deecke, J. E.; Sidjabat, H. E.; Ramaologa, S.; Zuegg, J.; Betley, J. R.; Beevers, A. P. G.; Smith, R. A. G.; Roberts, J. A.; Paterson, D. L.; Cooper, M. A. Protein-inspired antibiotics active against vancomycin- and daptomycin-resistant bacteria. *Nat. Commun.* **2018**, *9*, 22.

(14) Antonoplis, A.; Zang, X.; Huttner, M. A.; Chong, K. K. L.; Lee, Y. B.; Co, J. Y.; Amieva, M. R.; Kline, K. A.; Wender, P. A.; Cegelski, L. A dual-function antibiotic-transporter conjugate exhibits superior activity in sterilizing MRSA biofilms and killing persister cells. *J. Am. Chem. Soc.* **2018**, *140*, 16140−16151.

(15) Umstätter, F.; Domhan, C.; Hertlein, T.; Ohlsen, K.; Mühlberg, E.; Kleist, C.; Zimmermann, S.; Beijer, B.; Klika, K. D.; Haberkorn, U.; Mier, W.; Uhl, P. Vancomycin resistance is overcome by conjugation of polycationic peptides. *Angew. Chem., Int. Ed. Engl.* **2020**, *59*, 8823−8827.

(16) Guan, D.; Chen, F.; Qiu, Y.; Jiang, B.; Gong, L.; Lan, L.; Huang, W. Sulfonium, an Underestimated Moiety for Structural Modification, Alters the Antibacterial Profile of Vancomycin Against Multidrug-Resistant Bacteria. *Angew. Chem., Int. Ed. Engl.* **2019**, *58*, 6678−6682.

(17) Yarlagadda, V.; Sarkar, P.; Samaddar, S.; Haldar, J. A vancomycin derivative with a pyrophosphate-binding group: a strategy to combat vancomycin-resistant bacteria. *Angew. Chem., Int. Ed. Engl.* **2016**, *55*, 7836−7840.

(18) Jiang, Y.; Han, M.; Bo, Y.; Feng, Y.; Li, W.; Wu, J. R.; Song, Z.; Zhao, Z.; Tan, Z.; Chen, Y.; Xue, T.; Fu, Z.; Kuo, S. H.; Lau, G. W.; Luijten, E.; Cheng, J. "Metaphilic" cell-penetrating polypeptide-vancomycin conjugate efficiently eradicates intracellular bacteria via a dual mechanism. *ACS Cent. Sci.* **2020**, *6*, 2267−2276.

(19) Okano, A.; Isley, N. A.; Boger, D. L. Peripheral modifications of [Ψ[CH2NH]Tpg4]vancomycin with added synergistic mechanisms of action provide durable and potent antibiotics. *Proc. Natl. Acad. Sci. U.S.A.* **2017**, *114*, E5052−E5061.

(20) Wu, Z.-C.; Isley, N. A.; Boger, D. L. N-terminus alkylation of vancomycin: ligand binding affinity, antimicrobial activity, and site-specific nature of quaternary trimethylammonium salt modification. *ACS Infect. Dis.* **2018**, *4*, 1468−1474.
(21) Printsevskaya, S.; Reznikova, M.; Korolev, A.; Lapa, G.; Olsufyeva, E.; Preobrazhenskaya, M.; Plattner, J.; Zhang, Y. Synthesis and study of antibacterial activities of antibacterial glycopeptide antibiotics conjugated with benzoxaboroles. *Future Med. Chem.* **2013**, *5*, 641−652.
(22) Karlowsky, J. A.; Nichol, K.; Zhanel, G. G. Telavancin: mechanisms of action, in vitro activity, and mechanisms of resistance. *Clin. Infect. Dis.* **2015**, *61*, S58−S68.
(23) Sarkar, P.; Samaddar, S.; Ammanathan, V.; Yarlagadda, V.; Ghosh, C.; Shukla, M.; Kaul, G.; Manjithaya, R.; Chopra, S.; Haldar, J. Vancomycin derivative inactivates carbapenem-resistant Acinetobacter baumannii and induces autophagy. *ACS Chem. Biol.* **2020**, *15*, 884−889.
(24) Allen, N. E.; Nicas, T. I. Mechanism of action of oritavancin and related glycopeptide antibiotics. *FEMS Microbiol. Rev.* **2003**, *26*, 511−532.
(25) Ghosh, C.; Manjunath, G. B.; Akkapeddi, P.; Yarlagadda, V.; Hoque, J.; Uppu, D. S. S. M.; Konai, M. M.; Haldar, J. Small molecular antibacterial peptoid mimics: the simpler the better! *J. Med. Chem.* **2014**, *57*, 1428−1436.
(26) Wu, Z.-C.; Isley, N. A.; Okano, A.; Weiss, W. J.; Boger, D. L. C1-CBP-vancomycin: impact of a vancomycin C-terminus trimethylammonium cation on pharmacological properties and insights into its newly introduced mechanism of action. *J. Org. Chem.* **2020**, *85*, 1365−1375.
(27) Wenzel, M.; Kohl, B.; Münch, D.; Raatschen, N.; Albada, H. B.; Hamoen, L.; Metzler-Nolte, N.; Sahl, H.-G.; Bandow, J. E. Proteomic response of Bacillus subtilis to lantibiotics reflects differences in interaction with the cytoplasmic membrane. *Antimicrob. Agents Chemother.* **2012**, *56*, 5749−5757.
(28) Strahl, H.; Hamoen, L. W. Membrane potential is important for bacterial cell division. *Proc. Natl. Acad. Sci. U.S.A.* **2010**, *107*, 12281−12286.
(29) Scherer, K. M.; Spille, J.-H.; Sahl, H.-G.; Grein, F.; Kubitscheck, U. The lantibiotic nisin induces lipid II aggregation, causing membrane instability and vesicle budding. *Biophys. J.* **2015**, *108*, 1114−1124.
(30) Hurdle, J. G.; O'Neill, A. J.; Chopra, I.; Lee, R. E. Targeting bacterial membrane function: an underexploited mechanism for treating persistent infections. *Nat. Rev. Microbiol.* **2011**, *9*, 62−75.
(31) Tamer, Y. T.; Toprak, E. On the race to starvation: how do bacteria survive high doses of antibiotics? *Mol. Cell* **2017**, *68*, 1019−1021.
(32) Keren, I.; Kaldalu, N.; Spoering, A.; Wang, Y.; Lewis, K. Persister cells and tolerance to antimicrobials. *FEMS Microbiol. Lett.* **2004**, *230*, 13−18.
(33) Moormeier, D. E.; Bayles, K. W. Staphylococcus aureusbiofilm: a complex developmental organism. *Mol. Microbiol.* **2017**, *104*, 365−376.
(34) Hall-Stoodley, L.; Costerton, J. W.; Stoodley, P. Bacterial biofilms: from the natural environment to infectious diseases. *Nat. Rev. Microbiol.* **2004**, *2*, 95−108.
(35) Parsek, M. R.; Singh, P. K. Bacterial biofilms: an emerging link to disease pathogenesis. *Annu. Rev. Microbiol.* **2003**, *57*, 677−701.
(36) MacKenzie, F. M.; Gould, I. M. The post-antibiotic effect. *J. Antimicrob. Chemother.* **1993**, *32*, 519−537.
(37) Yarlagadda, V.; Konai, M. M.; Manjunath, G. B.; Prakash, R. G.; Mani, B.; Paramanandham, K.; Ranjan, S. B.; Ravikumar, R.; Chakraborty, S. P.; Roy, S.; Haldar, J. In vivo antibacterial activity and pharmacological properties of the membrane-active glycopeptide antibiotic YV11455. *Int. J. Antimicrob. Agents* **2015**, *45*, 627−634.
(38) O'Driscoll, T.; Crank, C. W. Vancomycin-resistant enterococcal infections: epidemiology, clinical manifestations, and optimal management. *Infect. Drug Resist.* **2015**, *8*, 217−230.
(39) Bender, J. K.; Cattoir, V.; Hegstad, K.; Sadowy, E.; Coque, T. M.; Westh, H.; Hammerum, A. M.; Schaffer, K.; Burns, K.; Murchan, S.; Novais, C.; Freitas, A. R.; Peixe, L.; Del Grosso, M.; Pantosti, A.; Werner, G. Update on prevalence and mechanisms of resistance to linezolid, tigecycline and daptomycin in enterococci in Europe: Towards a common nomenclature. *Drug Resist. Updates* **2018**, *40*, 25−39.
(40) Epand, R. M.; Epand, R. F. Bacterial membrane lipids in the action of antimicrobial agents. *J. Pept. Sci.* **2011**, *17*, 298−305.
(41) Romaniuk, J. A.; Cegelski, L. Bacterial cell wall composition and the influence of antibiotics by cell-wall and whole-cell NMR. *Philos. Trans. R. Soc. B* **2015**, *370*, 20150024.
(42) Zheng, E. J.; Stokes, J. M.; Collins, J. J. Eradicating bacterial persisters with combinations of strongly and weakly metabolism-dependent antibiotics. *Cell Chem. Biol.* **2020**, *27*, 1544−1552 e3.
(43) Yarlagadda, V.; Samaddar, S.; Paramanandham, K.; Shome, B. R.; Haldar, J. Membrane disruption and enhanced inhibition of cell-wall biosynthesis: a synergistic approach to tackle vancomycin-resistant bacteria. *Angew. Chem., Int. Ed. Engl.* **2015**, *54*, 13644−13649.
(44) Yarlagadda, V.; Sarkar, P.; Manjunath, G. B.; Haldar, J. Lipophilic vancomycin aglycon dimer with high activity against vancomycin-resistant bacteria. *Bioorg. Med. Chem. Lett.* **2015**, *25*, 5477−5480.
(45) Yarlagadda, V.; Akkapeddi, P.; Manjunath, G. B.; Haldar, J. Membrane active vancomycin analogues: a strategy to combat bacterial resistance. *J. Med. Chem.* **2014**, *57*, 4558−4568.
(46) Konai, M. M.; Ghosh, C.; Yarlagadda, V.; Samaddar, S.; Haldar, J. Membrane active phenylalanine conjugated lipophilic norspermidine derivatives with selective antibacterial activity. *J. Med. Chem.* **2014**, *57*, 9409−9423.
(47) Te Winkel, J. D.; Gray, D. A.; Seistrup, K. H.; Hamoen, L. W.; Strahl, H. Analysis of antimicrobial-triggered membrane depolarization using voltage sensitive dyes. *Front. Cell Dev. Biol.* **2016**, *4*, 29.
(48) Stulke, J.; Hanschke, R.; Hecker, M. Temporal activation of -glucanase synthesis in Bacillus subtilis is mediated by the GTP pool. *J. Gen. Microbiol.* **1993**, *139*, 2041−2045.

https://doi.org/10.1021/acs.jmedchem.1c00449
J. Med. Chem. 2021, 64, 10185−10202